communications earth & environment

Article

A Nature Portfolio journal

https://doi.org/10.1038/s43247-026-03417-y

Temperature-driven decline in recalcitrant dissolved organic carbon weakens coastal macrophyte's blue carbon storage potential

Alba Yamuza-Magdaleno [1] ✉, Tomás Azcárate-García [2,3], Luis Gonzalo Egea [1], Xosé Antón Álvarez-Salgado [4], Hauke Reuter [5], Fernando Guillermo Brun [1,6] & Pedro Beca-Carretero [4,5,6] ✉

Marine macrophytes, including seagrasses and seaweeds, are major contributors to the marine carbon cycle through the release of dissolved organic carbon, a fraction of which is recalcitrant (resistant to microbial degradation for weeks to months), thereby supporting long-term carbon storage. Here we tested how warming and invasion by a non-native seagrass affect carbon dynamics in temperate macrophyte communities from southern Iberia using controlled mesocosm experiments across three temperatures. The invasive seagrass did not substantially alter carbon metabolism or dissolved organic carbon release. However, warming altered the amount and composition of released carbon. The recalcitrant fraction decreased by 28% with increasing temperature, while labile carbon (readily degradable) increased proportionally. When standardized to macrophyte carbon stocks, the recalcitrant fraction produced was comparable to sediment carbon burial rates in the same communities. These results suggest that warming restructures dissolved organic carbon composition, reducing coastal carbon storage capacity and affecting global carbon budget estimates.

Marine ecosystems play a pivotal role in the global carbon cycles, with coastal and oceanic habitats contributing to climate regulation through efficient CO_2 capture and long-term storage[1,2]. Seagrasses, mangroves, and salt marshes are recognized as key blue carbon ecosystems that bury organic matter (OM) in sediments, potentially sequestering carbon for centuries to millennia[3–5]. Macroalgae contribute to carbon cycling by producing abundant biomass, part of which is exported as organic carbon to deep habitats via lateral advection and subsequent sinking, a pathway also associated with seagrasses, salt marshes, and mangroves[6–9]. Phytoplankton drive the biological carbon pump through CO_2 fixation and export of organic carbon via vertical mixing of dissolved and suspended OM, and sinking of particulate OM, including zooplankton fecal pellets[10–13], sequestering carbon in abyssal layers for long timescales[14].

Despite the well-established pathways of particulate carbon burial and export, the fate of carbon released as dissolved organic carbon (DOC) (i.e., the fraction of marine OM lower than 0.2–0.7 μm[15]; remains poorly understood. DOC fractions span a broad reactivity spectrum from labile (lifetime of hours–days) to ultra-refractory forms (lifetime tens of millennia)[16]. Authors by agreement denote as 'labile' (LDOC) the fraction of DOC that is utilised by microbial communities rapidly (i.e., which does not accumulate in seawater), while the fraction that shows resistance to rapid OM decay and is accumulated at different timescales in seawater is considered as 'recalcitrant' (RDOC)[16]. Recent studies recorded both fractions in the macrophytes-derived DOC, highlighting the RDOC as an overlooked pathway in the contribution of macrophytes to ocean carbon sequestration[17–20]. However, the inclusion of macrophytes-derived RDOC as a feasible nature-based solution into blue carbon initiatives is still at an early stage of research since (i) the limited number of data of DOC degradation from macrophytes beyond few days or weeks[20]; (ii) the lack of a standardized framework regarding the units utilized to show these fluxes (so far appear

[1]Department of Biology, Division of Ecology, Faculty of Marine and Environmental Sciences, University of Cadiz, Puerto Real, Spain. [2]Department of Marine Biology and Oceanography, Institute of Marine Sciences (ICM-CSIC), Barcelona, Spain. [3]Department of Evolutionary Biology, Ecology and Environmental Sciences & Biodiversity Research Institute (IRBio), University of Barcelona, Barcelona, Spain. [4]Department of Oceanography, Institute of Marine Research (IIM-CSIC), Vigo, Spain. [5]Programme Area Ecosystem Co-Design towards a sustainable Anthropocene, Leibniz Centre for Tropical Marine Research, Bremen, Germany. [6]These authors contributed equally: Fernando Guillermo Brun, Pedro Beca-Carretero. ✉e-mail: alba.yamuza@uca.es; pbeca@iim.csic.es

normalized by dry/fresh biomass, surface area, volume, mol of oxygen, grams of carbon, etc in the literature) which hinder the comparison among marine communities and among compartment within the coastal carbon cycle; and (iii) the gaps of knowledge regarding possible changes on macrophytes DOC dynamics under both, current and future climate conditions[21]. For instance, warming affects the oceanic DOC cycle by enhancing both its production and the microbial degradation of recalcitrant compounds[21–24]. Notably, a 1 °C increase can lead to a 15–18% rise in the degradation rates of the recalcitrant fractions that turns over in decades, potentially reducing the global ocean DOC reservoir by ~7 Pg C[23]. Overall, both DOC composition and temperature are key factors controlling its degradation, with higher temperatures consistently accelerating decay rates[25]. These findings primarily refer to the open ocean, where DOC pools are relatively well characterized. By contrast, little is known about how DOC dynamics respond to warming in coastal ecosystems, where DOC production and degradation are more variable and closely tied to benthic primary producers[26].

Phytoplankton, macroalgae, and seagrasses are major DOC contributors, exporting globally ~11.54, 8.46, and 4.52 mol C m^{-2} yr^{-1}, respectively[9,10,27]. DOC released by primary producers and the balance between labile and recalcitrant fractions are influenced by the physiological state (e.g., growth phase and stress), species-specific traits (e.g., size and growth rate), and environmental factors such as temperature, light, and nutrient availability[28–32]. The quantity and composition of DOC released by marine photosynthetic organisms are partially modulated by their species-specific thermal responses. Under optimal or near-optimal thermal conditions, DOC release may decline (e.g., *Zostera marina*[33]; *Ecklonia radiata*[34]. In contrast, under suboptimal or stressful warming conditions, species may release more DOC (e.g., *Cymodocea nodosa*[18,27]; *Laminaria digitata*[35]. In phytoplankton, experimental warming of +2 to +6 °C above their optimal temperature range led to a higher DOC release[36]. These contrasting results underscore the species-specific and thermal context-dependent nature of DOC responses to temperature. Moreover, DOC fluxes are influenced by organism size and ecological strategy. Smaller, fast-growing species typically release a higher fraction of DOC relative to biomass. For instance, picoplankton release 15–30% vs. < 10% in larger phytoplankton[37,38]. Relative to the lability of DOC, small macrophyte species likely release more LDOC relative to their biomass, while larger species might produce structurally more carbon linked to RDOC forms[39].

Global warming and biological invasions are notably reshaping marine ecosystems, particularly in temperate and subtropical regions. Native seagrasses such as *Cymodocea nodosa* and *Zostera noltei*, and macroalgae such as *Caulerpa prolifera*, are adapted to thermal ranges of approximately 5–28 °C but are experiencing increasing stress and habitat contraction due to rising sea surface temperatures in the Mediterranean and eastern Atlantic[40,41]. Simultaneously, the tropical seagrass *Halophila stipulacea*, native to the Red Sea and Indian Ocean, is rapidly expanding into these warming habitats, often displacing native species such as *C. nodosa*[42–46], also interacting with native macrophytes like *Z. noltei* and *Caulerpa* spp.[47–49]. A critical knowledge gap persists regarding how the co-occurrence and interaction between native and invasive macrophyte species affect biogeochemical processes, particularly the production, composition, and persistence of DOC[17].

Accurately quantifying DOC fluxes, especially its recalcitrant fraction, is essential to understand the role of coastal vegetated ecosystems in ocean carbon cycling and long-term carbon storage[50]. However, the lack of experimental studies assessing different pathways of carbon sequestration in representative seagrass beds (e.g., comparing carbon burial in sediments and rates of carbon export as RDOC in situ) and the lack of a standardized framework regarding the units utilized to show these fluxes are hindering not only the comparison among marine communities, but also to provide reliable estimations of contribution of seagrass-derived RDOC in ocean carbon sequestration. For instance, DOC production is typically normalized to fresh biomass or surface area in marine macrophyte studies[21,27,51], but rarely normalized to dry weight, internal carbon content, or chlorophyll content[52]. By contrast, DOC production is usually tied to volume, chlorophyll content or internal carbon budgets in phytoplankton studies, yet RDOC-specific rates are rarely quantified[53–55]. This constraint also prevents direct cross-system comparisons among different primary producer communities, such comparing DOC production rates of seagrasses versus phytoplankton. Another poorly defined aspect in the assessment of bacterial DOC consumption, and, by extension, the distinction between LDOC and RDOC, is the wide variability in incubation periods used across studies. Reported durations range from 15 to over 60 days[18,20,25,39,56], introducing major uncertainty in the comparability and interpretation of results, since shorter incubation periods may overestimate the proportion of RDOC[57,58]. This issue is exacerbated by the absence of standardized criteria for defining and isolating RDOC fractions, which can differ widely in bioavailability and yield time calculations and estimations depending on environmental context and methodological approach.

To investigate how metabolic and DOC-related parameters of temperate seagrass communities are affected by global change stressors, and to address methodological gaps in DOC flux estimations, the objectives of this study are: (i) To assess whether temperature and the presence of an invasive species influence metabolism and DOC fluxes in temperate marine macrophytes, and to quantify daily DOC (labile and recalcitrant) production rates relative to dry weight, internal carbon content of living tissues, and chlorophyll content; and (ii) To establish a standardized methodology for comparing DOC and RDOC production with sedimentary carbon accumulation rates and to enable cross-ecosystem comparisons among different primary producer communities, such as seagrasses, seaweeds, and phytoplankton. We hypothesize that warming and invasive species pressures will increase respiration rates in seagrasses and macroalgae, favouring RDOC release over LDOC. We further propose that this RDOC pool, often overlooked in blue carbon assessments, constitutes a key component of marine carbon sinks, with annual contributions comparable to long-term sedimentary carbon burial.

Material and methods

Study Sites and sampling strategy

The rising of ocean temperature is facilitating the spread of *Halophila stipulacea* through the Mediterranean Sea and along the Atlantic coast of the Caribbean Sea[42,46,59–61]. Thus, this species is starting to reach areas inhabited by more template macrophyte species, recording its coexistence with *Cymodocea nodosa* and *Posidonia oceanica*[41,62], as well as the macroalgae *Caulerpa* spp.[49,63] in some locations. To a lesser extent, it coexists with *Zostera noltei*[45,48]. For this reason, we conducted our experiments on mixed macrophyte communities representative of Atlantic and Mediterranean temperate ecosystems, also including the tropical invasive seagrass species *H. stipulacea*. The temperate species *C. nodosa*, *Z. noltei*, and *C. prolifera* were collected from the Bay of Cadiz (southern Spain; 36°29'21.0"N, 6°15'53.6"W), a transitional area between Atlantic and Mediterranean marine climate regimes with water temperatures ranging from 13 °C to 24 °C, reaching up to 28 °C in heat waves. For additional information on the study area, review previous studies of the Bay of Cadiz[64,65]. The invasive species *H. stipulacea* was collected from Mayagüez Bay, Puerto Rico (18°12'36.4"N, 67°09'41.1"W). Mayagüez Bay is a tropical coastal ecosystem within the Caribbean Sea, characterized by warm tropical conditions and the presence of seagrass species such as *Thalassia testudinum*, *Syringodium filiforme*, and *Halophila ovalis*. Surface water temperatures in this region typically range from 24 °C to 30 °C year-round. Shoots from both sites were manually harvested by snorkelling at 1–2 m depth in June and July 2023. Sampling was conducted at regular 5–10 m intervals along a 50 m transect to minimize collecting shoots from the same clone/genotype. Collected shoots were transported within 30 h to the Marine Experimental Facilities (MAREE) at the Leibniz Centre for Tropical Marine Research (ZMT) in Bremen, Germany. During transport, shoots were wrapped in seawater-moistened tissue, placed in plastic bags, and packed in insulated coolers to maintain moist, cool conditions.

Experimental Setup

The experiment was conducted for 25 weeks (Supplementary Fig. S1) in a large mesocosm facility composed by 27 aquaria (300 L, 58 cm wide, 80 cm long, and 65 cm high each aquarium) at ZMT's MAREE facility. Each system included a recirculating setup (Supplementary Fig. S2) with biological filtration (1 g filter media per 10 L water) and mechanical filtration, operating at ~60 L h^{-1} to achieve five full water turnovers daily. Three months prior to macrophyte transplantation, a 6 cm sediment layer of aragonite sand (80% medium-grain: 1.7 mm; 20% fine-grain: 0.75 mm; 1.87 ± 0.1% organic matter (OM)) was placed in each aquarium. A commercial bacterial solution (Fauna Marin Bacto Blend) was introduced to stimulate microbial colonization, and systems were stabilized for three months to develop mature microbial communities in sediments and filters. In parallel, each aquarium was inoculated with wet sediment from the Bay of Cadiz (10–20% of the aquarium's sediment) to introduce native temperate microbial and bacterial assemblages. Weekly, 20% of the water was replaced with artificial seawater (Red Sea Salt; 36 PSU salinity). Nutrients were supplemented to maintain ~3 µM nitrate, ~1 µM ammonium and ~0.2 µM phosphate concentrations, replicating natural habitat conditions at the Bay of Cadiz in summer[31]. Fluorescent lighting maintained an irradiance of 300 µmol photons m^{-2} s^{-1} at the sediment surface under a 12 h light:dark cycle, simulating natural light conditions in the donor area[66]. Salinity, pH, and dissolved oxygen were monitored weekly using a conductivity sensor (TetraCon 925), pH sensor (SenTix 980), and optical oxygen sensor (FDO925), respectively (Supplementary Fig. S3). Nutrient concentrations were analyzed weekly in parallel (Supplementary Table S1). To reduce algal growth, epiphytes on aquarium walls were manually removed every 2–3 days.

Following transplantation in June, all species underwent an acclimation period of six weeks (June–July 2023) to allow plants to recover and start growing new tissue in the aquaria (Supplementary Fig. S4A). *Halophila stipulacea* transplants underwent an additional step-wise temperature acclimation because water temperature at collection time in Puerto Rico was ~28 °C. That is, shoots were held initially at 28 °C for 2 weeks, then 26 °C for 2 weeks, and finally 24 °C for 2 weeks before the starting of the experiment. This gradual procedure acclimated *H. stipulacea* to the base temperature of our treatments (24 °C) without temperature shock. The native species from Cadiz were maintained at ~24 °C (their average summer temperature) during this period. To transition from 24 °C to the elevated treatments, we increased temperatures gradually over 7 days (~ 0.5 °C per day up to 28 °C). In order to ensure physical isolation between species while minimizing interference with the growth of each, the species within each aquarium were separated using PVC dividers (Supplementary Fig. S2). Consequently, approximately 6 g fresh weight (FW) of each species were introduced per aquarium, with an average density of 41 shoots of each species per aquarium.

The experimental warming treatments were initiated in August 2023 and ran for six weeks (to mid-September 2023). We used a fully factorial design with temperature (three levels) and community (three levels). Temperature treatments were: (i) 24 °C (control, current summer conditions), (ii) +2 °C (26 °C, moderate warming), and (iii) +4 °C (28 °C, high warming). These values represent, in these Mediterranean-Atlantic communities, the upper thermal range they experience in situ, from colder (Atlantic) to warmer areas in central and eastern Mediterranean Sea. Community treatments were: (i) Native control (the three native species together), (ii) *H. stipulacea* control, and (iii) Native + *H. stipulacea* mixed (interaction) (Supplementary Fig. S4B). Each of the 3 × 3 temperature × community combinations were replicated in triplicate ($N = 27$ aquaria). Aquaria were randomly arranged to avoid spatial biases in light or room conditions. Temperature in each aquarium was regulated by independent-aquarium heaters and chillers, closely monitored; during the experiment, temperatures stayed within ± 0.2 °C of targets.

Benthic chambers were installed in each compartment of the aquaria on day 21 (midpoint of the temperature and community experiment) to conduct metabolism and DOC measurements (Supplementary Fig. S5). Each benthic chamber (~ 2 L) consisted of a polyvinyl chloride (PVC) cylinder (~ 8 cm diameter, 10 cm height, 0.0064 m^2) attached to an airtight polyethylene bag (~ 40 cm height, 15 cm width), following designs used in previous macrophyte studies[17,67,68]. The PVC cylinder had a sharpened lower edge to allow full insertion into the sediment (6 cm deep) while avoiding damage to macrophyte leaves. Each polyethylene bag included a sampling port in the upper half (~ 30 cm) for water collection. The flexible walls (~ 0.07 mm thick) allowed natural movement with water flow, preventing stagnation.

The ratio of fresh biomass (g FW) relative to water volume (liter) used for benthic chambers was established based on preliminary experiments testing different biomass-to-water ratios across incubation times of 1, 3, 6, 12, 24, 36, and 72 h. Based on these trials, a ratio of 1–2 g of aboveground biomass (AG) per liter of water was identified as optimal for a 24-hour incubation period. This proportion was selected to prevent saturation of DOC in the incubation. Fresh biomass (g FW) was measured immediately after the 18 h incubation. Once the full experiment was completed, the fresh-to-dry biomass ratio was calculated and applied to the fresh weight to estimate dry weight used in the metabolism and DOC experiments (Supplementary Table S2). The analysis of the biomass data introduced into the benthic chambers (including *C. nodosa*, *Z. noltei*, *C. prolifera*, and *H. stipulacea* species) yielded a mean total biomass value of approximately 0.212 g dry weight (DW) inside the chambers in the experiment. Given the chamber surface area, the biomass-to-surface area ratio of the mesocosm meadows ranged from 30 to 40 g DW m^{-2}. The carbonate-rich sediment used in all aquaria was homogenized prior to the experiment and its OM content was quantified to ensure that any DOC released from sediment-associated OM should be comparable across treatments. For that, sediment subsamples in each benthic chamber ($n = 66$) were taken from the top centimeters of the sediment to analyze the OM content (~ 2.09 ± 0.02% DW; Supplementary Table S2) using the loss-on-ignition method in an oven at 550 °C for 5 h (Supplementary Table S2). No significant differences were found among aquaria.

DOC flux estimates were then normalized to plant dry weight (AG and total biomass), internal carbon content (carbon content in biomass), and total chlorophyll content (the sum of chlorophyll *a* and *b*). To establish these relationships, at the end of the experiment all plant material from each benthic chamber was harvested to determine AG and belowground (BG) biomasses (g DW m^{-2}, dried at 60 °C for 48 h). Subsamples of this biomass were analyzed for carbon and pigment contents (Supplementary Tables S2, S3). We used a CHN analyzer (PerkinElmer 2400) to measure carbon and nitrogen in plant tissues (~ 7 mg of freeze-dried, ground biomass per sample, combusted at 900 °C[69]). Pigments were extracted following protocols established in previous studies[70]: ~20–30 mg of powdered freeze-dried leaf tissue was mixed with 5 mL of 100% methanol, kept in the dark at 4 °C for 20 h with constant stirring. After centrifugation, the clarified extract was stored at 4 °C in the dark. Chlorophyll *a*, chlorophyll *b*, and total carotenoids were then measured with a UV-Vis spectrophotometer (Agilent Cary 50) according to traditional equations developed in previous studies[71]. Equations 1–3 in Supplementary Information (SI).

Photosynthetic efficiency

Each week, we assessed morphometric and physiological indicators of plant performance (Supplementary Table S4). Measurements were conducted repeatedly on the same tagged individual within each aquarium whenever possible, allowing temporal tracking of individual-level responses across the experimental period. Growth metrics included leaf elongation rate (cm day^{-1}), new shoot/frond production (% increase), and rhizome elongation (cm day^{-1}). Plant physiological status was evaluated via chlorophyll fluorescence (maximum quantum yield, F_v/F_m). In situ F_v/F_m was measured at night on 3–5 leaves per species per aquarium using a Diving-PAM fluorometer (Walz, Germany). These values were then compared to those from field-collected specimens of the same species: the temperate species with populations from the Bay of Cadiz, and for *H. stipulacea*, mesocosm values were compared to nearby natural populations from the Caribbean Sea[72].

Carbon metabolism

Following methods used in previous studies[32,33], dissolved oxygen (DO) in each benthic chamber was measured at three times spanning a daily cycle: just before sunset (S1), immediately after sunrise (S2), and six hours after sunrise (S3) (Supplementary Fig. S5A), which allow to differentiate metabolic rates during both dark and light periods. Specifically, DO concentrations were measured by collecting water samples from inside the benthic chambers using acid-washed 50 mL syringes (standard plastic, prevalidated through blank controls). Water was slowly introduced into glass vials to prevent the formation of bubbles. Each vial was equipped with a self-adhesive oxygen sensor dot (OXSP5-ADH, PyroScience). An adapter was attached to the outside of the vial to ensure contact between the sensor and a fiber optic with an integrated lens (SPFIB-LNS, PyroScience). The temperature in each benthic chamber was recorded using a temperature sensor (TSUB21, PyroScience). Both the SPFIB-LNS and TSUB21 sensors were connected to a FireSting-O_2 fiber-optic oxygen meter (PyroScience), which had an integrated battery, LCD display, and logger. This system was used to record DO concentration (mg L^{-1}) and in situ temperature (°C) for O_2 calibration at 60-second intervals until readings stabilized.

Changes in DO concentration between the three sampling times (S1, S2, and S3) were used to calculate net primary production (NPP) and respiration (R), which were then used to estimate gross primary production (GPP). The chosen time spans are standard for this methodology[51,67,73], and are sufficient to detect DO changes while avoiding DO oversaturation in the incubators. However, it is possible that NPP may be slightly underestimated due to the isolation of the communities within the benthic chambers. This limitation suggests that the community's autotrophic capacity could be higher than indicated by our current results[51,67,74]. Hourly rates of R, NPP and GPP were calculated using equations 4–7 in SI.

Metabolic rates in DO units were converted to carbon units using photosynthetic (PQ = moles O_2: moles CO_2) and respiratory quotients (RQ) of 1, values commonly applied in seagrass meadows studies[75–77]. These equations and calculations are standard in published research on carbon metabolism[17,51,67].

Dissolved Organic Carbon (DOC) fluxes

To calculate DOC fluxes, water samples were collected from the benthic chambers using 50 mL acid-washed syringes at the same S1, S2, and S3 sampling times as community carbon metabolism measurements (Section "Experimental Setup"). Approximately 20 mL of each sample was filtered (precombusted GF/F, 47 mm), fixed with 0.08 mL of 30% H_3PO_4 in acid-washed glass vials sealed with silicone-Teflon caps. Samples were stored in the dark until analysis. DOC concentrations were determined using at high temperature catalytic oxidation (720 °C) in a Shimadzu TOC-VCPH analyzer at the Institute of Marine Research (INMAR) at University of Cadiz (Spain).

The net DOC flux was calculated as the difference between final and initial DOC concentrations in the water samples, following protocols established by previous studies[67,73,78]. Hourly DOC flux rates during night and light periods were derived using established equations 8–10 in SM.

Daily DOC flux rates were calculated as the sum of the hourly DOC flux in light multiplied by light hours (12 h) and the hourly DOC flux in night multiplied by night hours (12 h). Thus, when net DOC flux was positive, the community was considered to act as a net DOC source, while when net DOC flux was negative, the community behaved as a net DOC sink.

DOC Bioavailability: Labile and Recalcitrant DOC Production

To evaluate the bioavailability of DOC produced by different benthic communities under varying temperature and interaction conditions (Supplementary Fig. S4A), we performed a DOC degradation assay following the initial measurements of DO and DOC (Sections "Carbon metabolism" and "Dissolved Organic Carbon (DOC) fluxes"). Following the names of earlier works[17,18,79], we use the term 'recalcitrant' fraction of DOC (RDOC) to refer to the remaining fraction of DOC at the end of bioavailability assay. Likewise, the term 'labile' fraction of DOC (LDOC) refers to the fraction of DOC that is utilized by heterotrophic bacteria during the assay (i.e., the difference between the initial DOC concentration and RDOC).

From each aquarium, 300 mL of seawater were collected from the benthic chambers using 50 mL acid-washed syringes. For the native control and interaction treatments, 100 mL were taken from the chamber corresponding to each species and pooled (300 mL total) to integrate DOC production across the entire community. To prepare the incubation medium, 270 mL of the pooled water were filtered through 0.2 µm polycarbonate filters to remove bacteria while allowing DOC to pass. Later, a volume of 30 mL of water (bacteria inoculum) from in situ natural communities were filtered through 0.8 µm filters to retain larger particles but preserving the natural bacterial community (i.e., retain bacteria). These fractions were combined into hermetically sealed 300 mL glass bottles. A total of 27 incubation beakers (one for each replicate of each treatment) were prepared and incubated in darkness at a constant temperature of 18 °C. The DOC bioavailability assay was run for 60 days, allowing sufficient time for LDOC to be consumed and the system to reach a stationary phase, as previously reported for macrophyte-derived DOC[17,80]. DOC decay rate (k) during the assay was modelled using a first-order exponential decay equation with two DOC pools, LDOC and RDOC (ref. 25; Equation 11 in SI).

Water samples were collected at the following times: 0, 1, 3, 7, 15, 30, 45, and 60 days, and at each time DOC was measured. Initial DOC concentration (C_0) was measured after addition of the bacterial inoculum. Control tests indicated that the inoculum's DOC contribution was negligible and did not influence estimates of degradation kinetics. Notably, to prevent the onset of anaerobic processes during bacterial inoculation, it was essential to maintain a molar excess of oxygen relative to the final amount of carbon present after 60 days of incubation. This ensured that carbon consumption occurred exclusively through aerobic metabolic pathways, allowing us to confirm that all assimilated carbon was processed under strictly aerobic conditions. After 60 days, the percentage reduction of DOC from its initial value was considered the LDOC fraction, while the remaining DOC was categorized as the no labile fraction, which we used as the RDOC fraction of macrophyte-derived DOC (Equations 12–13, SI).

DOC production rates relative to Plant Biomass, Carbon Content, Chlorophyll Content and yield times

Daily production rates of LDOC and RDOC from biomass (AG and total) were calculated by multiplying the daily net DOC flux standardized per unit of biomass (g C g DW^{-1} d^{-1}, as calculated in Section "Dissolved Organic Carbon (DOC) fluxes") by the corresponding DOC fraction (%, labile or recalcitrant) (Equations 14–15, SI). This resulted in daily LDOC and RDOC release rates per unit biomass.

Yield times (in days) reflects the number of days required to generate 1 g of DOC from the available carbon content in biomass. Using the daily DOC production (g C g DW^{-1} d^{-1}) and the measured carbon content in biomass (g C g DW^{-1} in AG and total tissues), we estimated the yield times for net DOC, RDOC, and LDOC (equations 16–18, SI).

Based on the calculated DOC production rates and the measured carbon content in biomass (g C g DW^{-1}), we estimated how much DOC can be produced per day from 1 g of structural carbon in the plant biomass (daily DOC from carbon content in biomass, Equation 19 in SI). This normalization allows direct comparison of DOC release to the internal carbon content of the plants. Daily production rates of LDOC and RDOC were calculated by multiplying daily net DOC fluxes standardized per carbon content in biomass (g C g C^{-1} d^{-1}) by the corresponding fraction (labile or recalcitrant) (Equations 20–21, SI).

Daily Production Rates of DOC fractions were also calculated using the total chlorophyll content (Chl *a* plus *b*) of the plants, by multiplying net daily DOC fluxes standardized per unit of chlorophyll content (g C g Chl^{-1} d^{-1}) by the corresponding fraction (labile or recalcitrant) (Equations 22–23, SI). Although Chl is not the most commonly used indicator in macrophytes, we normalized DOC production to Chl content to enable comparisons with

other primary producer compartments, such as phytoplankton, where this metric is commonly used.

Comparison Across Carbon Pathways and Ecosystems

To evaluate distinct blue carbon pathways, we first compared DOC production rates from this study and DOC production rates measured in the same southern Iberian Peninsula macrophyte beds (*C. nodosa*, *Z. noltei*, *C. prolifera*) with sediment organic carbon burial rates measured in the same locations[18,66,81–83]. In addition, we compiled literature data on sediment carbon burial rates (g C m^{-2} yr^{-1}), AG biomass (g DW m^{-2}), and total biomass (AG and BG; g DW m^{-2}) for global macrophyte ecosystems (Supplementary Tables 5, 6). Using these carbon-related estimates, we derived annual organic carbon burial rates normalized to either AG or total biomass, expressed as g C g DW^{-1} yr^{-1} with the equation 24 in SI.

To estimate carbon-content-normalized burial rates (g C g C^{-1} yr^{-1}), we applied a mean carbon content in biomass value derived from our four study species to all taxa in the dataset (Supplementary Table S2). This approximation enabled a consistent comparison across species where direct carbon content in biomass measurements were unavailable (Equation 25 in SI).

Data and statistical analysis

All results were reported as mean ± standard error (SE) for replicated aquaria ($n = 3$ per treatment). We employed a combination of univariate and multivariate statistical approaches to analyze our data. To test main effects of Temperature, Community, and their interaction on carbon metabolism variables, we first applied two-way ANOVA when assumptions of normality and homogeneity were met; this included variables such as F_v/F_m, leaf growth, shoots/fronds production/elongation, DOC fluxes, and DOC bioavailability. For metrics not meeting these assumptions, we used non-parametric alternatives: Kruskal-Wallis tests for comparisons such as light versus night DOC differences, or rank transformation followed by factorial ANOVA (ART-ANOVA) for carbon metabolism rates, *k*, labile/recalcitrant DOC fractions, and DOC production rates. Where significant differences emerged, we conducted post-hoc comparisons using Tukey's HSD tests for parametric analyses or pairwise Wilcoxon tests for non-parametric analyses to examine specific group-level differences.

To isolate the effect of temperature (as a continuous variable) across community treatments, we performed Arrhenius-type linearization for metabolic rates and DOC fluxes, as well as conducting linear regression analyses with temperature for *k* and DOC fractions. For relationships where variables contained measurement error, such as between respiration and night-time DOC flux, we implemented Deming regression instead of ordinary least squares. This method accounts for uncertainty in both X and Y variables, unlike standard linear regression that assumes an error-free predictor, thereby providing more robust, symmetric relationship estimates under realistic field conditions.

Additionally, to visualize multivariate community-level patterns, we conducted non-metric multidimensional scaling (NMDS) ordination using the metaMDS() function from R's vegan package. This analysis incorporated a suite of variables including DOC fluxes and percentages of labile versus recalcitrant DOC, configured with two dimensions ($k = 2$), no data transformation, and a maximum of 100 iterations. We evaluated ordination fit using stress values, where values < 0.05 indicated excellent representation, and used PERMANOVA to formally test for multivariate treatment differences.

All analyses were executed in R (v4.0.2). Statistical significance was set at $\alpha = 0.05$, with results at $0.05 < \alpha < 0.1$ considered as marginal trends.

Results

Comparison between experimental and natural conditions of macrophytes

F_v/F_m results from our experimental individuals did not differ significantly from those in their natural environment (Supplementary Tables S4, S7). For example, *Cymodocea nodosa* in its natural area displayed F_v/F_m values of 0.81 ± 0.02, similarly to those observed in the experiment (0.79 ± 0.002). Regarding *Halophila stipulacea*, values of F_v/F_m did not display significant differences between experimental and field conditions (0.69 ± 0.01 and 0.69 ± 0.02, respectively). Similar values were also observed for *Caulerpa prolifera* and *Zostera noltei* in both the field and the mesocosm. In the case of *Z. noltei*, leaf growth in the mesocosm ranged from 0.08 to 0.18 cm d^{-1} (Supplementary Table S4), increasing from an initial length of 5.6 ± 0.3 cm to 6.3 ± 0.2 cm over the experimental period. No significant effects of temperature were observed on the morphometric and physiological characteristics of the plant (Supplementary Tables S8, S9).

Carbon Metabolism

The four macrophyte species clustered into two distinct groups based on carbon metabolic parameters (R, GPP, and NPP; Supplementary Figs. S6, S7 and Table S10,). *Cymodocea nodosa* and *C. prolifera* formed one group, while *Z. noltei* and *H. stipulacea* constituted the other, with the latter pair exhibiting significantly higher metabolic rates. *Cymodocea nodosa* and *C. prolifera* showed similar metabolic values when averaged across the three temperatures (24, 26, 28 °C). R in *C. nodosa* (2.66 ± 0.29 mmol C g DW^{-1} d^{-1}) did not differ significantly from R in *C. prolifera* (2.10 ± 0.39 mmol C g DW^{-1} d^{-1}), but both were markedly lower than the R values observed in *Z. noltei* (34.96 ± 6.51 mmol C g DW^{-1} d^{-1}) and *H. stipulacea* (21.15 ± 2.47 mmol C g DW^{-1} d^{-1}). Similar patterns were observed for GPP and NPP (Fig. 1, Supplementary Fig. S6).

Temperature had no significant effect on any of the metabolic rates when all community treatments and species were considered together (Supplementary Table S11), although there was a marginal trend for R to increase with temperature ($p = 0.1$; Supplementary Table S10). When each species was analyzed separately, NPP tended to decrease with rising temperature for all species; this decline was most pronounced in *C. prolifera* ($p = 0.06$; Supplementary Table S12). Overall, when native species (*C. nodosa*, *Z. noltei*, and *C. prolifera*) were grown in interaction with *H. stipulacea*, no significant temperature effects were observed on any of the metabolic rates. The average NPP of native species under control conditions (6.64 ± 2.95 mmol C g DW^{-1} d^{-1}) was significantly lower than that of *H. stipulacea* under control conditions (18.62 ± 6.53 mmol C g DW^{-1} d^{-1}). Nonetheless, when each species was evaluated independently, NPP did not differ between individuals grown alone (control) and those grown in interaction with *H. stipulacea*.

Dissolved Organic Carbon (DOC) fluxes

DOC fluxes were significantly higher during the daylight hours than at night across all community treatments (native control, *H. stipulacea* control, and the interaction community) (Supplementary Table S13). Overall, temperature had no significant effect on DOC fluxes measured during night, light, or over a full day (Supplementary Tables S11, S14, S15). However, when community treatments were analyzed individually, *H. stipulacea* under control conditions showed a significant decrease in night DOC flux with increasing temperature, dropping from 0.12 ± 1.19 mmol C g $DW^{-1}h^{-1}$ at 24 °C to −2.77 ± 0.64 mmol C g $DW^{-1}h^{-1}$ at 28 °C (Fig. 2A, Supplementary Table S16). Regarding light DOC fluxes, temperature did not significantly affect any community treatment (Fig. 2B). The native control tended to increase light DOC production with rising temperature, however the *H. stipulacea* control and the interaction treatment did not report a clear pattern. These outcomes were also reflected in daily net DOC fluxes (Fig. 2C).

When averaging temperature treatments, DOC fluxes did not differ significantly among the three community treatments, except at night. During the night period, the *H. stipulacea* control treatment had a significantly lower mean DOC flux (−1.34 ± 0.83 mmol C g $DW^{-1}h^{-1}$) compared to the interaction treatment (0.07 ± 0.08 mmol C g $DW^{-1}h^{-1}$) (Fig. 2A, Supplementary Table S14). A positive correlation was also observed between night DOC fluxes and respiration (Supplementary Fig. S8).

DOC bioavailability

The DOC pool exhibited a significant 1st-order decay trend over the 60-day bioavailability assay across all temperature treatments (Supplementary

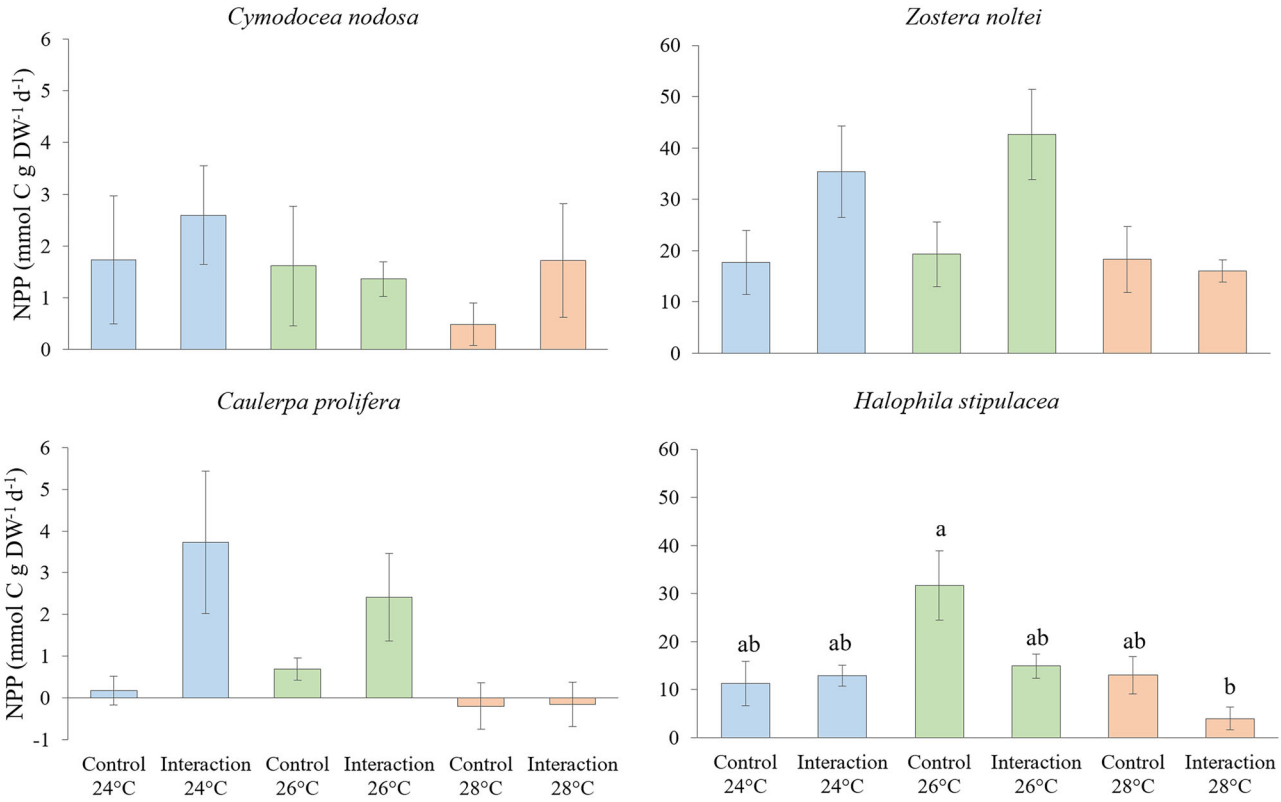

Fig. 1 | Interactive effects of temperature and invasive species on daily net primary production across macrophyte species. Daily rates (mean ± SE, $n = 3$, error bars represent the standard error of the mean) of net primary production (NPP) in the four studied species (*Z. noltei, C. nodosa, C. prolifera* and *H. stipulacea*) and different temperatures: 24 °C (blue), 26 °C (green), and 28 °C (orange). Letters above the bars indicate significant differences among temperature and community treatments of the same species ($p < 0.05$).

Table S17). On average, microbial degradation accounted for 51%, 56%, and 65% of the initial DOC at 24, 26, and 28 °C (Fig. 3), respectively. Incubations using DOC from the 28 °C treatments had significantly lower percentages of DOC remaining at day 60, indicating a lower recalcitrant DOC fraction in those treatments (Supplementary Tables S18, S19). However, irrespective of temperature, no significant differences were observed among the three community treatments (native control, *H. stipulacea* control, and interaction) in the percentage of DOC remaining at day 60. These temperature-driven shifts in recalcitrant DOC proportion occurred despite minimal changes in metabolic rates (Section "Carbon Metabolism"), highlighting a decoupling between whole-community carbon metabolism and DOC bioavailability responses.

Linear regression revealed a significant relationship between temperature and the k of DOC produced at various temperatures across all community treatments ($y = 163.4 - 5.63x$; $R^2 = 0.307$; $p = 0.003$; Supplementary Table S11). This indicates a clear decline in k from 24 °C to 28 °C (Fig. 4; Supplementary Tables S20, S21, S22), with the results being much more dispersed at 24 °C. Similarly, analyzing each community treatment separately (native control, *H. stipulacea* control, interaction) revealed that all showed a decreasing trend in k with warming (Supplementary Table S23). Notably, k declined faster with rising temperatures, even though the DOC released under these conditions contained a greater proportion of labile carbon (Section 3.4.3).

Overall, temperature had a significant effect on both labile and recalcitrant DOC fractions across all community treatments (Supplementary Table S11). As temperature increased, the proportion of LDOC produced by the communities increased significantly, while the fraction of recalcitrant DOC decreased (Fig. 5A). Significant differences in both DOC fractions were observed between 24 °C and 28 °C ($p = 0.02$; Supplementary Table S22). The lowest recalcitrant DOC fraction was observed in the interaction treatment at 28 °C (31 ± 2%), whereas the highest was observed in the native control at 24 °C (65 ± 15%) (Fig. 3). Despite these temperature-driven changes, the different community treatments did not differ significantly from each other when temperature was not considered. The average recalcitrant DOC fractions (across all temperatures) were 46 ± 10% for the native control, 46 ± 3% for the *H. stipulacea* control, and 45 ± 7% for the interaction.

In addition, non-metric multidimensional scaling (NMDS) of the DOC fluxes and bioavailability data showed a clear ordination of samples by temperature (Supplementary Fig. S9). Samples from the 28 °C treatments clustered tightly, indicating consistent behaviour across replicates, whereas samples at 24 °C were more variable, which is also observed in Fig. 4B. The stress value was 0.015, indicating an excellent ordination fit.

DOC production and yield times

DOC production rates per AG biomass (g C g DW^{-1} d^{-1}) tended to increase with temperature across all community treatments (native control, *H. stipulacea* control, and interaction), with this pattern being more evident in the native control (Table 1, Supplementary Fig. 10, and Tables S11, S24). This trend was observed for net and for recalcitrant, and labile DOC fractions. In contrast, DOC yield times tended to decrease with increasing temperature, with a marginally significant trend observed for the yield time of LDOC ($p = 0.08$). Similarly, DOC production rates normalized to the carbon content in AG biomass also increased with temperature, with a marginally significant effect for LDOC ($p = 0.08$). There were no significant differences in DOC production or yield times among the three community treatments at any given temperature.

DOC production rates per total biomass (AG and BG, g C g DW^{-1} d^{-1}) showed trends consistent with those observed for AG biomass (Supplementary Figs. S10, S11), although statistical support was marginal for both net ($p = 0.09$) and labile ($p = 0.07$) DOC production rates (Table 1 and Supplementary Table S11). When normalized to the carbon content in total

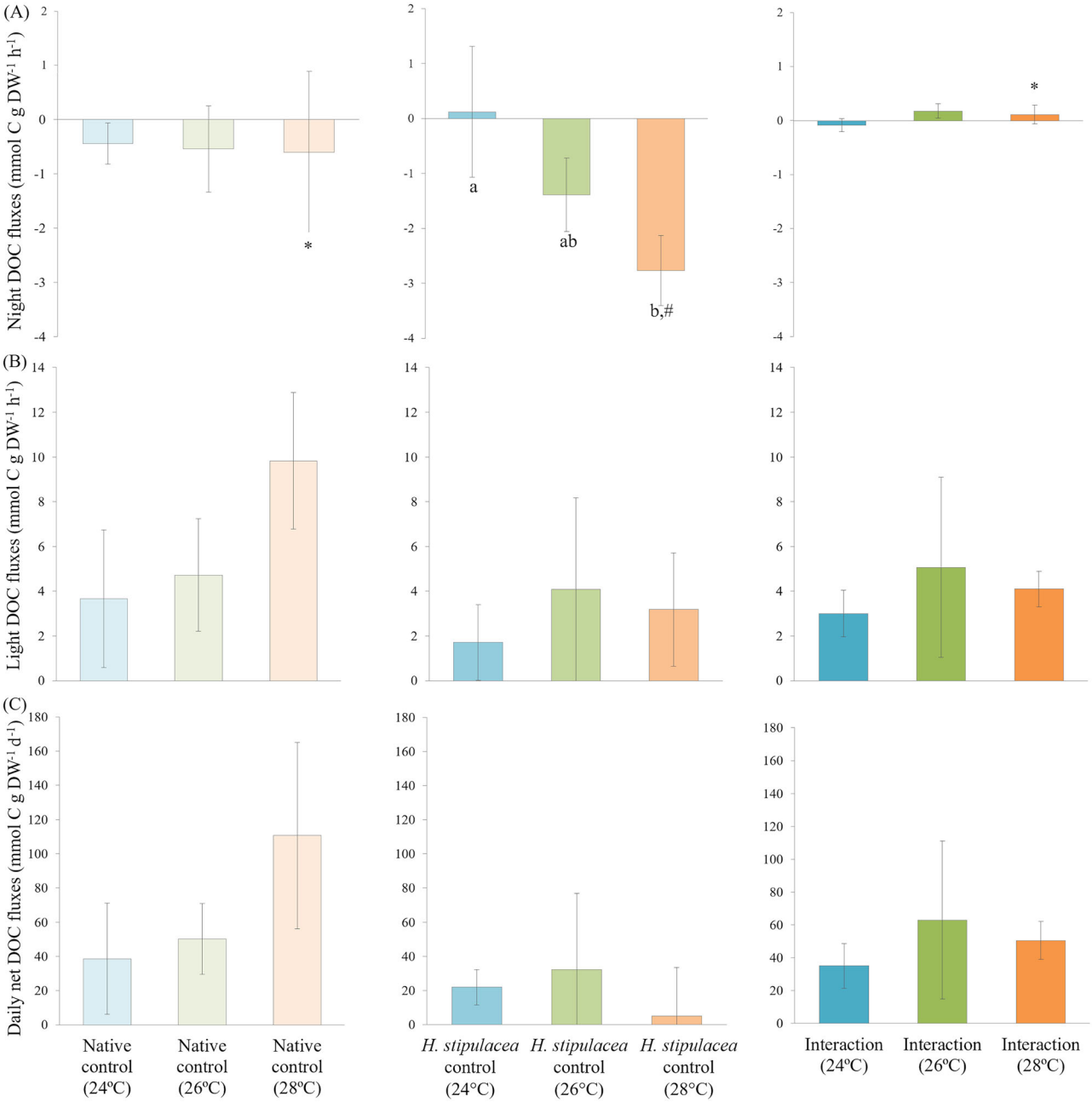

Fig. 2 | Interactive effects of temperature and invasive species on DOC fluxes. DOC fluxes (mean ± SE, $n = 3$, error bars represent the standard error of the mean) measured during (**A**) night hours, (**B**) light hours, and (**C**) net daily (24 h) fluxes across different treatments. The Native control represents the mean flux from the three native species (*Z. noltei, C. nodosa, C. prolifera*) together. The *H. stipulacea* control includes fluxes only from *H. stipulacea*. The Interaction treatment is the mixed community of natives + *H. stipulacea*. Each community treatment was evaluated under 24 °C (blue), 26 °C (green), and 28 °C (orange). Letters above bars denote significant differences between temperatures within a given treatment ($p < 0.05$). Symbols (*, #) indicate significant differences between community treatments at a given temperature.

biomass, the daily net DOC production rate was found to be around 0.26 g Cg $C^{-1}d^{-1}$ (including all community and temperature treatments). This means that these communities required ~3.9 days to produce an amount of DOC equivalent to their carbon biomass.

The mean daily net DOC production per carbon content in total biomass (grouping the values of the three community treatments, native control, *H. stipulacea* control and interaction) at 24 °C and 28 °C was 0.13 ± 0.02 and 0.31 ± 0.07 g C g C^{-1} d^{-1}, respectively (Supplementary Fig. S11). Both daily net and labile DOC production rates per carbon content in total biomass increased significantly with temperature ($p = 0.046$ and $p = 0.03$, respectively; Supplementary Table S11 and Fig. S6C). Similarly, the daily recalcitrant DOC production rates per C content in total biomass at 24 °C and 28 °C were 0.06 ± 0.01 and 0.11 ± 0.02 g Cg $C^{-1}d^{-1}$, respectively, which implies an 83% more carbon production at 28 °C than at 24 °C. It does allow for the quantification of temperature-enhanced recalcitrant carbon output in relation to carbon content in biomass.

In addition, regardless of temperature, species under interaction conditions showed a 55% increase in recalcitrant DOC production rates per carbon content in total biomass compared to those under control conditions (from 0.09 ± 0.03 g Cg $C^{-1}d^{-1}$ at control conditions to 0.05 g Cg $C^{-1}d^{-1}$ in interaction with *H. stipulacea*; Fig. 6 C). Again, no significant effect of temperature or community on yield times was found (Supplementary Fig. S11 and Table S24).

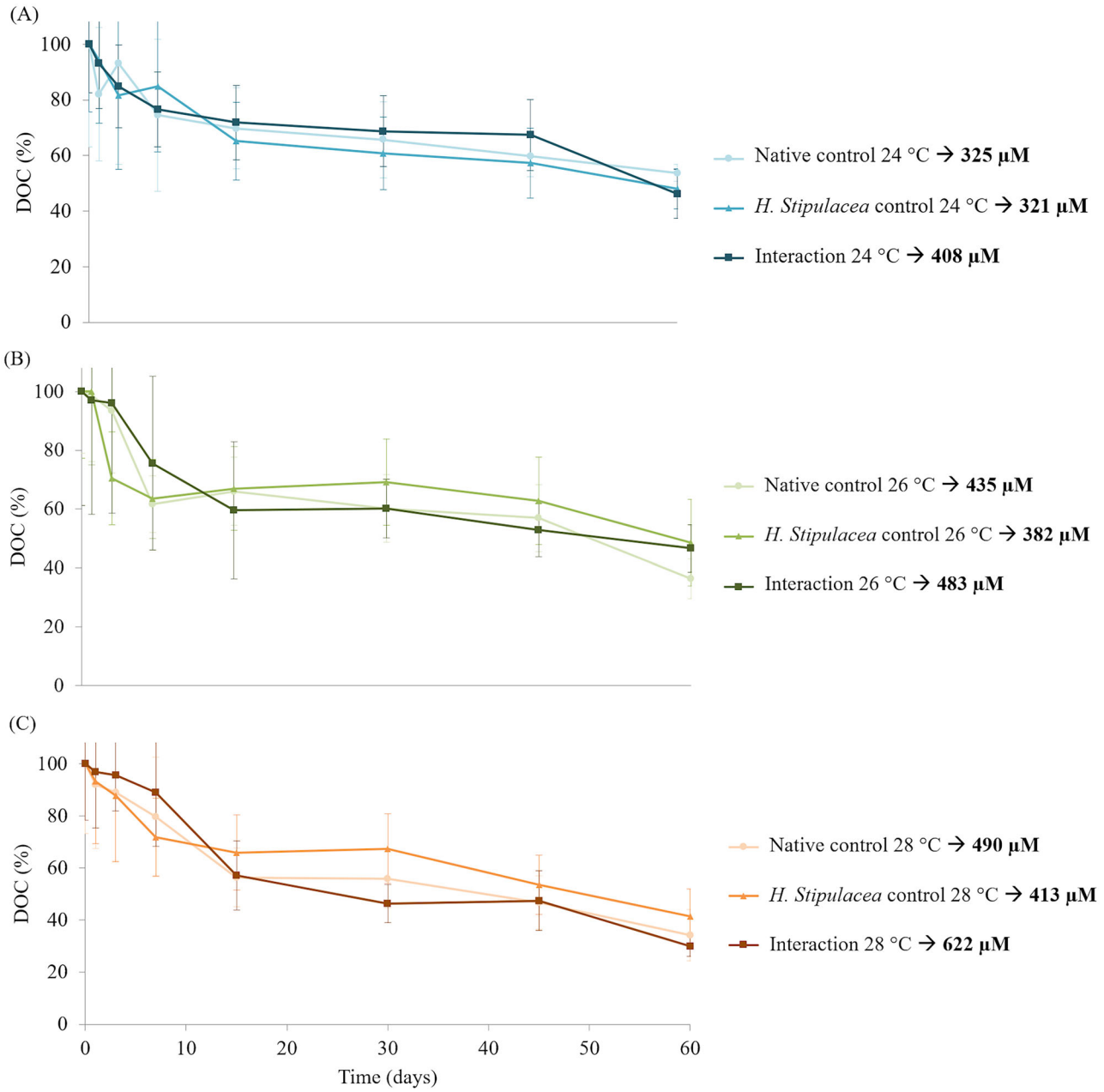

Fig. 3 | Bioavailability assays using DOC samples collected at the end of the mesocosm incubations. Each panel shows the DOC decay (mean ± SE, $n = 3$, error bars represent the standard error of the mean) over 60 days for the (**A**) 24 °C, (**B**) 26 °C, and (**C**) 28 °C treatments, for DOC derived from the Native control, *H. stipulacea* control, and Interaction communities. Data are expressed as remaining DOC (% of initial concentration) ± SE ($n = 3$). The values in the legend indicate the initial DOC concentrations (µM) at the start of the bioassay for each community treatment.

Finally, DOC production rates calculated based on total chlorophyll content showed similar trends to those based on biomass and carbon content in biomass (Supplementary Fig. S12 and Table S11). However, none of these chlorophyll normalized trends was statistically significant.

Discussion

Carbon Metabolism, DOC Fluxes and Production Rates

Across the experimental thermal range, temperature increases did not notably affect the photosynthetic efficiency (F_v/F_m) of studied marine macrophytes, either relative to natural ambient conditions in the Mediterranean and Atlantic seas. These results were in the same range as those of other studies that analyzed the same species[84–86]. The mean biomass of the mesocosm was found to be approximately 30–40 g DW m^{-2}. A review of the literature (Supplementary Tables S5, S6) indicates that this ratio falls within the range reported for other seagrass meadows worldwide (at the lower end of the range), suggesting that the experimental conditions reproduced realistic natural biomass densities, although in the lower limit. Experimental warming produced subtle reductions in net productivity alongside slightly respiration rises (Fig. 1, S5). Previous studies have shown that warming typically stimulates metabolic processes and respiration in autotrophic organisms, enhancing photosynthesis performance[87–89]. However, in our experiment favorable warming conditions generated distinct metabolic responses among the macrophyte species, likely reflecting species-specific ecological strategies and thermal acclimation capacity. The four species clustered into two metabolic groups, *Z. noltei* (native) and *H. stipulacea* (invasive) had substantially higher R, GPP, and NPP compared to *C. nodosa* (native) and *C. prolifera* (native), which showed much lower rates (Fig. 1, S5,

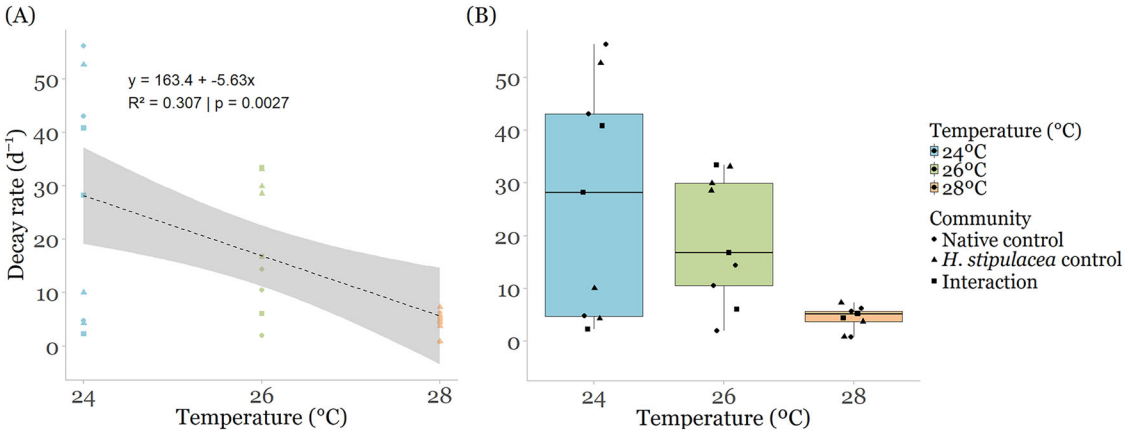

Fig. 4 | Effect of temperature on DOC decay rate (k) ($n = 9$). **A** Linear regression of *k* vs. temperature, across the three community treatments. Points represent individual observations, the dashed line shows the linear regression fit, and the shaded area indicates the 95% confidence interval. **B** Boxplots of *k* at each experimental temperature, showing distribution of k values in each community treatment. Boxes represent the interquartile range (IQR), centre lines indicate medians, and whiskers extend to the most extreme data point within 1.5 × IQR; points show individual observations. Community treatments: Native control (circles), *H. stipulacea* control (triangles), and Interaction (squares). Temperature treatments: 24 °C (blue), 26 °C (green), 28 °C (orange).

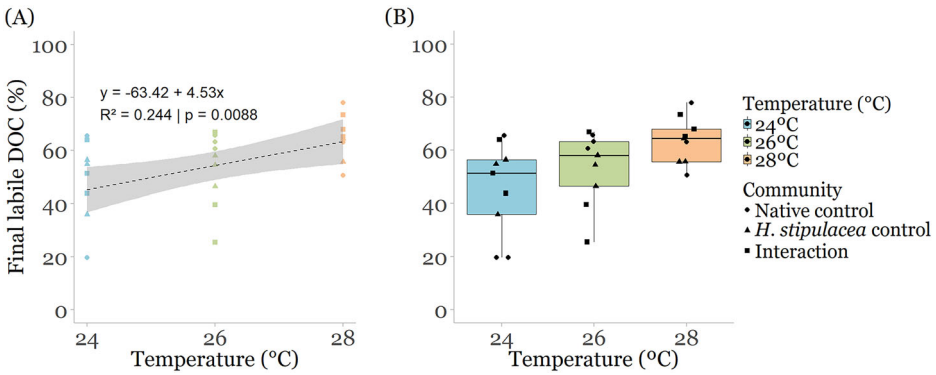

Fig. 5 | Effect of temperature on final fractions of labile DOC (%) ($n = 9$). **A** Linear regression showing a relationship between temperature and labile DOC fraction across the three community treatments. Points represent individual observations, the dashed line shows the linear regression fit, and the shaded area indicates the 95% confidence interval. **B** Boxplots of DOC fractions at each experimental temperature treatment, illustrating the distribution of values for each community treatment. Boxes represent the interquartile range (IQR), centre lines indicate medians, and whiskers extend to the most extreme data point within 1.5 × IQR; points show individual observations. Community treatments: Native control (circles), *H. stipulacea* control (triangles), and Interaction (squares). Temperature treatments: 24 °C (blue), 26 °C (green), 28 °C (orange).

S6). *Zostera noltei* exhibited notably higher R, GPP, and NPP than co-occurring species, along with a 10–20% increase in shoot size, indicating enhanced metabolic performance and substantial growth under experimental conditions. In contrast, *C. nodosa* and *C. prolifera* appeared to prioritize resource conservation, as neither species significantly increased nor decreased their body size over the course of the experiment. *Halophila stipulacea* showed no significant changes in metabolic parameters across the temperature range, consistent with its pioneer strategy characterized by high thermal plasticity and rapid biomass turnover that supports its fast colonization of diverse environments[62].

Notably, daily net DOC fluxes were positive across all treatments, indicating that the community functioned as a net DOC source as already found in other macrophyte species[67]. Temperature influenced both, the quantity and composition of DOC exuded by macrophytes, with higher net DOC release during light hours either in native or invasive communities. This pattern, consistent with previous macrophyte studies[27,66], reflects the strong link between DOC release and photosynthetic activity. According to the stoichiometric overflow hypothesis, released DOC is related to surplus photosynthate production under high photosynthetic conditions and particularly under nutrient limitation[90]. The native macrophyte community showed a clear temperature-dependent increase in DOC production, with daily net release rates nearly tripling from 24 °C to 28 °C, while *H. stipulacea* exhibited no consistent thermal response (Fig. 2). This aligns with previous findings that favorable warming conditions within a species' thermal optimum can enhance DOC exudation[27,88], as also observed for *C. nodosa* under short-term warming during summer season[51], accompanied by an overall rise in both labile and recalcitrant DOC (LDOC and RDOC) production rates. However, in our study, with increasing temperature, the relative proportion of LDOC rose while the proportion of RDOC declined significantly, with an average reduction of ~7% in the RDOC fraction per 1 °C warming (approximately a 28% total decrease from 24 °C to 28 °C; Supplementary Table S11, Fig. 5). These findings are particularly noteworthy as they suggest that warming conditions within their optimal of temperature enhances the production of labile carbon fraction, yet alters their balance, favoring the production of labile carbon compounds that are more readily assimilable by bacteria. Changes in DOC composition driven by temperature likely reflect shifts in internal carbon allocation between photosynthetic production and respiratory demand, as well as changes in the microbiome and how organic matter (OM) in water and sediment is processed. Respect to macrophytes, warming conditions may stimulate photosynthesis within the species' thermal optimum, increasing the availability of photosynthates and favoring the release of more labile compounds[91,92]. In contrast, higher respiratory costs at elevated temperatures can divert carbon toward maintenance metabolism and the synthesis of more complex or stress-related molecules, which tend to contribute to the recalcitrant DOC pool[35,36,93–95]. This is likely due to the production of more respiration-derived, humic, and other complex

https://doi.org/10.1038/s43247-026-03417-y

Table 1 | DOC production rates per aboveground (AG) and total (AG + BG) biomasses, yield times, and DOC production rates per carbon content in biomass (AG and total) for each community treatment (Native control, *H. stipulacea* control, and Interaction) across temperatures (24 °C, 26 °C and 28 °C)

Community	Native control	*H. stipulacea* control	Interaction	Native control	*H. stipulacea* control	Interaction	Native control	*H. stipulacea* control	Interaction
Temperature	24 °C	24 °C	24 °C	26 °C	26 °C	26 °C	28 °C	28 °C	28 °C
Aboveground biomass									
Daily net DOC production rate per AG biomass (g C g DW^{-1} d^{-1})	0.46 ± 0.39	0.26 ± 0.13	0.42 ± 0.16	0.60 ± 0.25	0.85 ± 0.27	1.17 ± 0.41	1.33 ± 0.65	0.40 ± 0.03	0.61 ± 0.14
Daily labile DOC production rate per AG biomass (g C g DW^{-1} d^{-1})	0.28 ± 0.27	0.14 ± 0.07	0.23 ± 0.09	0.39 ± 0.17	0.44 ± 0.12	0.58 ± 0.34	0.89 ± 0.51	0.24 ± 0.03	0.42 ± 0.10
Daily recalcitrant DOC production rate per AG biomass (g C g DW^{-1} d^{-1})	0.18 ± 0.12	0.12 ± 0.05	0.19 ± 0.08	0.21 ± 0.08	0.41 ± 0.16	0.59 ± 0.17	0.44 ± 0.21	0.16 ± 0.01	0.18 ± 0.04
Net DOC yield time (days)	0.76	0.96	0.81	0.61	0.45	0.29	0.28	0.60	0.52
Labile DOC yield time (days)	1.25	1.77	1.51	0.94	0.87	0.59	0.41	1.01	0.74
Recalcitrant yield time (days)	1.93	2.10	1.74	1.70	0.92	0.58	0.84	1.45	1.71
Daily net DOC production rate per C content in AG biomass (g C g C^{-1} d^{-1})	1.37 ± 1.16	1.03 ± 0.48	1.23 ± 0.44	1.65 ± 0.70	2.19 ± 0.57	3.44 ± 1.12	3.74 ± 1.83	1.68 ± 0.13	1.93 ± 0.45
Daily labile DOC production rate per C content in AG biomass (g C g C^{-1} d^{-1})	0.83 ± 0.79	0.56 ± 0.29	0.67 ± 0.24	1.06 ± 0.47	1.15 ± 0.29	1.64 ± 0.89	2.49 ± 1.41	0.99 ± 0.13	1.34 ± 0.32
Daily recalcitrant DOC production rate per C content in AG biomass (g C g C^{-1} d^{-1})	0.54 ± 0.37	0.47 ± 0.20	0.56 ± 0.22	0.59 ± 0.23	1.04 ± 0.30	1.80 ± 0.64	1.25 ± 0.63	0.69 ± 0.02	0.59 ± 0.13
Total biomass									
Daily net DOC production rate per total biomass (g C g DW^{-1} d^{-1})	0.04 ± 0.03	0.03 ± 0.01	0.05 ± 0.02	0.07 ± 0.03	0.09 ± 0.03	0.14 ± 0.05	0.14 ± 0.07	0.04 ± 0.00	0.09 ± 0.02
Daily labile DOC production rate per total biomass (g C g DW^{-1} d^{-1})	0.02 ± 0.02	0.02 ± 0.01	0.03 ± 0.01	0.04 ± 0.02	0.05 ± 0.01	0.07 ± 0.04	0.09 ± 0.05	0.02 ± 0.00	0.06 ± 0.01
Daily recalcitrant DOC production rate per total biomass (g C g DW^{-1} d^{-1})	0.01 ± 0.01	0.01 ± 0.01	0.02 ± 0.01	0.02 ± 0.01	0.04 ± 0.02	0.07 ± 0.02	0.05 ± 0.02	0.02 ± 0.00	0.03 ± 0.01
Net DOC yield time (days)	8.80	7.85	6.07	5.04	3.52	2.27	2.36	4.98	3.25
Labile DOC yield time (days)	14.27	14.46	11.33	7.83	6.84	4.61	3.53	8.46	4.67
Recalcitrant DOC yield time (days)	22.99	17.16	13.07	14.13	7.26	4.48	7.13	12.14	10.71
Daily net DOC production rate per C content in total biomass (g C g C^{-1} d^{-1})	0.11 ± 0.10	0.13 ± 0.06	0.17 ± 0.07	0.20 ± 0.08	0.28 ± 0.07	0.44 ± 0.15	0.43 ± 0.21	0.20 ± 0.01	0.31 ± 0.07
Daily labile DOC production rate per C content in total biomass (g C g C^{-1} d^{-1})	0.07 ± 0.07	0.07 ± 0.04	0.09 ± 0.04	0.13 ± 0.05	0.14 ± 0.03	0.21 ± 0.12	0.29 ± 0.16	0.12 ± 0.01	0.21 ± 0.05
Daily recalcitrant DOC production rate per C content in total biomass (g C g C^{-1} d^{-1})	0.04 ± 0.03	0.06 ± 0.02	0.08 ± 0.04	0.07 ± 0.03	0.13 ± 0.04	0.23 ± 0.07	0.14 ± 0.07	0.08 ± 0.00	0.09 ± 0.02

Values are presented as mean ± SE.

compounds that are less accessible to bacterial communities[55]. On the other hand, temperature rise can swiftly reshape the microbial communities linked to seagrasses[96], often stimulating increases in bacterial density, activity, and respiration rates[97], which in turn may intensify the uptake of labile DOM by marine microbes. At the same time, microbial transformation of this labile material can result in the production of recalcitrant DOM, as shown in recent studies[19,79,98]. Although we did not directly measure metabolic intermediates or carbon partitioning, these mechanisms provide a plausible physiological framework that explains the observed reduction in RDOC proportion with warming. Our findings, therefore, challenge the commonly reported trends in marine primary producer communities. This raises a critical question: could warming conditions within their optimal range of temperature enhance the production of LDOC, while exceeding the thermal optimum induces physiological stress, shifting carbon partitioning toward more recalcitrant compounds? Interestingly, we also found that DOC k were lower at the highest temperature, indicating that newly released DOC was utilised by bacteria more rapidly when produced at lower temperatures. In other words, the effective bioavailability of the LDOC pool decreased as temperature increased within the optimal range. Thus, although warming enhanced DOC production and favoured the release of labile compounds, the bioavailability was lower at elevated temperature, resulting in an overall more RDOC pool at 28 °C. This temperature-dependent shift in DOC quality may have implications for carbon cycling and microbe–DOC interactions in coastal ecosystems under sustained warming scenarios. To the best of our knowledge this is the first time that k is applied in macrophyte studies.

The presence of the invasive species *H. stipulacea* had limited short-term effects on the native macrophyte community. We observed no significant changes in photosynthetic efficiency, metabolic rates, or DOC fluxes attributable to its presence. However, previous reports found that *H. stipulacea* negatively affected the growth and photosynthetic traits of *C. nodosa*[99], as well as field observations showing long-term impacts on native seagrass habitats[100,101]. To date, studies assessing how alien invaders influence carbon metabolism and DOC dynamics in macrophyte communities are scarce. Some studies reported that the invasion by the tropical macroalgae *Halimeda incrassata* in *C. nodosa* meadows decrease DOC release and shifted the balance toward more labile compounds in mixed communities[17]. In our experiment, DOC yield times, including net, labile, and recalcitrant fractions, were slightly lower in the presence of *H. stipulacea*. Several studies indicate that *H. stipulacea* may induce changes in sediment biogeochemistry, nutrient availability, carbon storage, and microbial community composition in the environments it colonizes[45,102]. A similar phenomenon occurs with *C. prolifera* species in Balearic Island (Spain). When it invades a *Posidonia oceanica* meadow, it modifies the sediment by releasing more DOC, altering hydrogen sulfide production, and changing the sediment's chemistry[103]. These alterations could partially explain the changes in the composition and lability of DOC released by the invaded community observed in our study.

This study provides the first quantification of LDOC and RDOC production rates normalized to plant carbon and total chlorophyll content in marine macrophytes. This approach allows to calculate DOC yield times. Our results evidenced the substantial release of DOC and RDOC that these species can reach under favorable conditions. When normalized to carbon content in total biomass, native species produced 0.25 g C g $C^{-1}d^{-1}$ of net DOC (corresponding to an average yield of ~4.1 days; Supplementary Table S25), while *H. stipulacea* produced 0.20 g C g $C^{-1}d^{-1}$ (yield ~4.7 days). Focusing on the RDOC, native species released 0.09 g C g $C^{-1}d^{-1}$ with a yield time of ~11.8 days, whereas *H. stipulacea* produced 0.10 g C g $C^{-1}d^{-1}$, with a yield of ~10.2 days. Temperature had a strong effect on DOC release rates. At 24 °C, native communities released 0.11 g $CgC^{-1}d^{-1}$ of net DOC (Table 1), corresponding to a yield time of 8.8 days, and 0.04 g C g $C^{-1}d^{-1}$ of RDOC with a yield time of ~23 days. At 28 °C, DOC production increased substantially: net DOC reached 0.43 g C g $C^{-1}d^{-1}$ (yield ~2.4 days), and RDOC increased to 0.14 g C g $C^{-1}d^{-1}$ with a reduced yield time of ~7.1 days (Table 1). These results highlight both the importance of incorporating carbon-normalized metrics in DOC studies and the temperature sensitivity of different DOC fractions, particularly the recalcitrant pool.

A Comparison of DOC Dynamics and Coastal Carbon Pathways

This study presents a standardized framework quantifying LDOC and RDOC production relative to carbon content in macrophyte biomass over defined time scales. This standardized approach facilitates direct comparisons with other carbon pathways, such as sedimentary organic carbon burial, and provides a foundation for consistent cross-ecosystem assessments among diverse primary producers (seagrasses, seaweeds, phytoplankton; Supplementary Tables S5, S6, S25).

We compared sediment carbon burial rates with DOC production rates obtained in our mesocosms within the same southern Iberian Peninsula macrophyte beds. For the native seagrass *C. nodosa*, annual sediment carbon burial was 0.53 g C g C^{-1} y^{-1}, while RDOC production reached 33.14 g C g C^{-1} y^{-1}, a difference of two orders of magnitude (Table 2 for *C. prolifera* and *Z. noltei* data). It is worth noting that recent incubations of *Zostera marina* leaves from Northern Spain under natural conditions, conducted over a full annual cycle, have reported net DOC production rates in the range of approximately 0.15–0.35 g C g $C^{-1}d^{-1}$, comparable to the values observed in the present study (Personal communication). Analysis of available literature data confirms that global organic carbon sequestration rates via burial in *C. nodosa* meadows (0.59 g C g C^{-1} y^{-1}; Supplementary Tables S5, S6) align closely with our local Iberian Peninsula observation (0.53 g C g C^{-1} y^{-1}). Using reported *C. nodosa* biomass (268 ± 54 g DW m^{-2}) and our DOC production metrics, we estimate that one square meter produces ~7.6 g C m^{-2} d^{-1} (~ 2.7 kg C m^{-2} y^{-1}; Table 2) of RDOC. This DOC flux is two orders of magnitude greater than the measured annual organic carbon burial rate in these productive meadows (0.039 kg C m^{-2}; Table 2).

It is essential to highlight that, when comparing our results with those obtained from previous field-based experiments, the DOC production rates of native species measured in mesocosms (0.25 g C g $C^{-1}d^{-1}$) were considerably higher, up to two orders of magnitude, than those reported for *C. nodosa* meadows in the Bay of Cadiz (0.004 g C g $C^{-1}d^{-1}$;[18]), as well as for other natural marine macrophyte communities[27]. There are several factors that could help explain the elevated DOC fluxes observed in our experiment. Notably, plant density in our mesocosm systems was lower than that found in natural seagrass meadows, which suggests that macrophyte biomass alone is unlikely to account for such high DOC production. In addition, the presence of epiphytes was minimal and did not contribute to overall metabolic activity. While the controlled mesocosm conditions, characterized by stable and optimal light, temperature, and nutrient levels, likely promoted continuous exudation of DOC by macrophytes and associated microbial communities, this does not fully explain the magnitude of DOC release recorded. Our DOC measurements aim to reflect the integrated exudation of the whole benthic community, including macrophytes, sediments, water and bacterial community, without isolating individual contributions, to quantify the integrated biogeochemical response of the entire benthic community, and to better represent natural ecosystem conditions.

A key factor may be the activity within the sediment compartment. In our experimental setup, the sediment was pre-conditioned and colonized over several months, allowing for the establishment of a mature microbial community in the absence of mechanical disturbances such as hydrodynamic forcing or bioturbation. The sediment OM content (~ 2.09 ± 0.02% DW; Supplementary Table S2) was comparable to values found in macrophyte-dominated coastal systems such as bays and estuaries[81], providing ample substrate for microbial degradation. Over the course of approximately 100 days, including the acclimation period, this microbial assemblage likely mineralized sedimentary OM at high rates. Moreover, experimental temperatures may have further stimulated microbial metabolism, as higher temperatures are known to enhance bacterial activity and OM turnover in sediments[104]. On the other hand, previous studies have shown that the DOC production of macrophytes of the same species can vary depending on whether they are found in muddy or sandy sediments[105]. The use of highly carbonated sediment in our mesocosms,

https://doi.org/10.1038/s43247-026-03417-y

Table 2 | Estimations of annual organic carbon (OC) burial rates and recalcitrant DOC production rates for each species of the Bay of Cadiz (*C. nodosa*, *Z. noltei*, *C. prolifera*) and *H. stipulacea*

Species	*C. nodosa*	*Z. noltei*	*C. prolifera*	*H stipulacea*	Average native species	Average native and invasive species
Organic carbon burial rates in natural communities						
Annual OC burial rate (g C m^{-2} y^{-1})	39.0 ± 0.0	62.0 ± 18.0	28.0 ± 0.0	10.44 ± 4.34	43.00 ± 10.02	34.86 ± 10.79
Annual OC burial rate per total biomass (g C g DW^{-1} y^{-1})	0.18 ± 0.00	0.27 ± 0.05	0.09 ± 0.00	0.33 ± 0.20	0.18 ± 0.05	0.22 ± 0.05
Annual OC burial rate per C content in total biomass (g C g C^{-1} y^{-1})	0.53 ± 0.00	0.91 ± 0.17	0.26 ± 0.00	1.29 ± 0.79	0.57 ± 0.19	0.75 ± 0.22
Recalcitrant DOC production rates in mesocosms communities						
Annual recalcitrant DOC production rate from total biomass (g C m^{-2} y^{-1})	2766.75 ± 949.05	2087.59 ± 716.09	3115.64 ± 1068.73	2804.56 ± 1020.45	2656.66 ± 301.83	2693.64 ± 216.61
Annual recalcitrant DOC production rate from C content in total biomass (g C m^{-2} y^{-1})	2903.67 ± 986.99	1909.63 ± 699.63	3367.64 ± 1207.59	434.07 ± 162.07	2726.98 ± 430.06	2153.75 ± 648.90
Annual recalcitrant DOC production rate per total biomass (g C g DW^{-1} y^{-1})	10.89	8.21	12.26	9.12 ± 3.52	10.45 ± 1.19	10.12 ± 0.90
Annual recalcitrant DOC production rate per C content in total biomass (g C g C^{-1} y^{-1})	33.14	25.00	37.32	33.25 ± 8.04	31.82 ± 3.62	32.18 ± 2.58
Recalcitrant DOC production rates in natural communities of the Bay of Cadiz						
Annual recalcitrant DOC production rate from total biomass (g C m^{-2} y^{-1})	44.29	44.74	25.82	29.76*	38.28 ± 6.23	36.15 ± 4.90
Annual recalcitrant DOC production rate from C content in total biomass (g C m^{-2} y^{-1})	133.31	134.68	77.72	89.59*	115.24 ± 18.76	108.83 ± 14.74
Annual recalcitrant DOC production rate per total biomass (g C g DW^{-1} y^{-1})	0.17	0.22	0.09	0.61*	0.16 ± 0.04	0.27 ± 0.12
Annual recalcitrant DOC production rate per C content in total biomass (g C g C^{-1} y^{-1})	0.50	0.67	0.26	1.84*	0.48 ± 0.12	0.82 ± 0.35
Net DOC production rates in natural communities of the Bay of Cadiz						
Annual net DOC production rate from total biomass (g C m^{-2} y^{-1})	98.4	99.43	57.38	66.14*	85.07 ± 13.85	80.34 ± 10.88
Annual net DOC production rate from C content in total biomass (g C m^{-2} y^{-1})	296.3	299.28	172.71	199.08*	256.10 ± 41.70	241.84 ± 32.75
Annual net DOC production rate per total biomass (g C g DW^{-1} y^{-1})	0.37	0.49	0.19	1.36*	0.35 ± 0.09	0.60 ± 0.26
Annual net DOC production rate per C content in total biomass (g C g C^{-1} y^{-1})	1.11	1.48	0.57	4.09*	1.05 ± 0.26	1.81 ± 0.78
Annual net DOC production rate per Chl content in biomass (g C g Chl^{-1} y^{-1})	183.62	270.74	108.85	679.73*	187.74	310.74
Recalcitrant DOC/OC burial rate	1.14	0.72	0.92	2.85	0.93 ± 0.12	1.41 ± 0.49
Literature sources for DOC flux estimates in natural communities	18,64,67	66	18	105		
Literature sources for OC burial rates in natural communities	81,82	81,82	81,82	116,117		

Values are presented as mean ± SE.

Values were calculated from the data of the mesocosms[118] and natural communities using biomasses extracted from the literature (Supplementary Tables S4 and S24).

*Since no published DOC fluxes data are currently available for *H. stipulacea*, values reported in for a seagrass meadow dominated by *H. australis*[105] have been used as a proxy.

combined with the presence of seagrasses, likely played a substantial role in the elevated DOC fluxes observed. Recent findings demonstrate that carbonate-associated OM (CAOM), a dynamic and exchangeable fraction of sedimentary organic carbon, can be released as DOC through carbonate dissolution processes[106]. These processes are often triggered by localized acidification and sulfide oxidation, both of which can be enhanced by oxygen transported into the sediment by seagrass roots. In our system, the activity of rooted macrophytes likely could promote aerobic microbial respiration and facilitating carbonate dissolution. Furthermore, the high porosity of the aragonite sediment may have enhanced oxygen penetration, reinforcing these processes[107]. As a result, the release of DOC in our experiment likely reflects not only direct exudation from plant biomass, but also the remobilization of sediment-bound OM. Altogether, these factors suggest that sediment microbial activity under controlled mesocosm conditions likely played a dominant role in driving the elevated DOC fluxes observed in this study.

Because the DOC release observed in our experimental setup was relatively high, we used field-based DOC production values to contextualize our findings and enable more robust comparisons with other macrophyte-related carbon cycle processes (e.g., sediment carbon burial) as well as with DOC production by other marine communities (e.g., macroalgae and phytoplankton). Based on values reported in earlier studies, net DOC production of *C. nodosa* in the donor area (i.e., Bay of Cadiz) correspond to an annual rate of 1.11 g C g $C^{-1}d^{-1}$[18,64,67]. Assuming that 45% of this DOC is recalcitrant, as suggested by our experimental findings, this would translate into a RDOC production of 0.50 g C g $C^{-1}d^{-1}$. This estimate is similar in magnitude to the annual carbon burial rate reported for *C. nodosa* in the Bay of Cadiz (0.53 g C g $C^{-1}d^{-1}$; Table 2,[81]). Notably, similar trends were observed for the other native species studied, *C. prolifera* and *Z. noltei* (Table 2). These findings further reinforce the potential relevance of RDOC as an important component of long-term carbon storage in coastal vegetated ecosystems. By extrapolating these results and taking into account the 36.15 g C m^{-2} y^{-1} (average annual RDOC production rate from total biomass, native/invasive; Table 2) as well as the worldwide estimated seagrass surface area (300,000–600,000 km^2;[75]), we found that macrophytes-derived RDOC may range 0.011–0.022 Gt C yr^{-1}. In the context of carbon burial, annual burial fluxes of 0.048 to 0.112 Gt C yr have been reported[3]. Consequently, the estimated annual flux of RDOC to the ocean's blue carbon pool appears to be at least in the same order of magnitude as the contribution from sediment carbon burial. Altogether, these findings underscore the importance of considering RDOC as a key component of the blue carbon pool, one that remains underrepresented in current carbon budgets and sequestration frameworks. However, the RDOC represents a poorly studied carbon pathway that warrants further investigation through expanded field and mesocosm studies, in order to compile robust datasets and refine future comparisons across species and ecosystems.

Our proposed framework also enabled comparisons of seagrass DOC production rates with those from other ecosystems, such as phytoplankton and macroalgae. When compared with macroalgae, net DOC production rates were found to be of a similar magnitude, with a rate of 4.26×10^{-4} g C g DW^{-1} d^{-1} reported for the green macroalgae *Caulerpa racemosa* (assuming an average biomass in the Mediterranean of 1,031.5 g DW m^{-2};[27,108]), in comparison with field studies for *C. nodosa* 3.04×10^{-4} g C g DW^{-1} d^{-1} (Table 2). Additionally, some studies have shown that phytoplankton can produce substantial amounts of DOC relative to chlorophyll content (between 0.05 and 10 g C g Chl^{-1} d^{-1};[53–55]), whereas transforming field data demonstrated that macrophytes generated DOC fluxes in the same order of magnitude (0.85 g C g Chl^{-1} d^{-1}). However, it's important to note that chlorophyll content may not be a consistent proxy for DOC production, as pigment concentrations are highly responsive to environmental factors such as light and temperature, potentially limiting their reliability as normalization metrics[109,110].

Importantly, our results show that 1 °C increase in temperature (from 24 °C to 28 °C) led to a 3.5–9% reduction in the release of RDOC by macrophytes. Similar trends have been observed in phytoplankton communities, where a 1 °C rise enhanced DOC degradation rates by 15–18%[23,24,111]. These findings support the idea that warming accelerates microbial activity, promoting the breakdown of recalcitrant compounds and potentially reducing the size of the ocean's DOC reservoir[112,113]. Notably, RDOC comprises 90–96% of the oceanic DOC pool and can persist for centuries to millennia[10,16], meaning that carbon entering this pool is effectively sequestered and removed from the rapid carbon cycle. Therefore, our findings suggest that seagrass and macroalgal meadows substantially contribute to this carbon sink as dissolved form, an overlooked component of blue carbon that remains underrepresented in global carbon inventories.

Methodological Insights and Limitations into DOC Production Rate Calculations

In this study, we propose a standardized framework to investigate DOC fluxes and production rates in vegetated coastal habitats. One of the most relevant innovations is the development of a quantitative framework that relates daily DOC production rates to the plant carbon and total chlorophyll contents. However, there are limitations in our proposed approach that should be acknowledged. First, the ~21 h incubations span full diel cycles during which bacterial consumption of LDOC occurs[114]. This prevents accurate estimation of gross DOC release, since a portion of the exuded DOC is remineralized during the incubation. Consequently, the values reported reflect net DOC accumulation and likely underestimate the actual release of bioavailable DOC. Second, the use of intact plant communities, including AG and BG tissues and associated microbiota, complicates the isolation of DOC derived solely from macrophyte metabolism[27]. Epiphytes, microbial assemblages, and sediment interactions contribute to DOC fluxes. In our biomass normalization, we did not include the biomass of associated organisms such as bacteria or epiphytes. Likewise, our method does not distinguish between DOC released from AG and BG tissues, even though these structures likely release distinct DOC fractions due to their physiological differences. It should also be noted that we did not separate DOC derived from macrophytes from DOC derived from sediments. However, the purpose of this study was to measure the integrated response of the benthic macrophyte community to warming and invasion. Therefore, it encompasses the combined effects of all system components, including macrophytes, sediment, the water column, and associated microbial communities. Nevertheless, all treatments began under uniform baseline conditions, with a standardized sediment inoculum and similar sediment OM content across aquaria. Therefore, the observed DOC fluxes reflect ecologically relevant, community-level responses to the applied stressors rather than processes specific to individual compartments. Lastly, our assessment of RDOC was conducted over 60 days, commonly a longer period than is typical in such studies (which often use 15–20 day bioassays)[18,21,39,115]. This extended incubation better captured LDOC consumption, but it does not imply that the remaining DOC is entirely inert over longer timescales. In fact, some of the DOC we classified as recalcitrant over 60 days could continue to break down on the scale of months to years[20]. Therefore, our RDOC should not be considered representative of ultra-refractory DOC, which remains preserved in the ocean for centuries to millennia. Although most of the bacterial consumption may have already occurred in our bioavailability assay, other chemical processes will continue to degrade the DOC, especially when considering longer-term degradation dynamics[39]. Despite the aim of this study was to evaluate the integrated response of the macrophyte community as a whole rather than to determine the basis of DOC production and composition, we acknowledge that future research should incorporate carbon-related metabolomics and stable isotope labeling. These approaches may clarify the specific metabolic pathways and sources that drive DOC composition and bioavailability under environmental stress. There are also inherent limitations in our laboratory setup. Despite the good condition of the macrophytes, we did not use an area that is fully representative of a natural population. As a result, our experimental system does not capture the full complexity of natural conditions, where additional biotic and abiotic processes may influence DOC dynamics. Therefore, the RDOC fractions we report should be treated with caution

when extrapolating to longer timescales. Despite these limitations, our results suggest that coastal vegetated habitats release considerable amounts of DOC that resist rapid microbial degradation, serving as a proxy for the RDOC fraction. The implementation of this standardized framework represents meaningful progress in quantifying DOC production in blue carbon systems and provides a solid foundation for future efforts to understand carbon fluxes in vegetated coastal ecosystems.

Conclusions

This study successfully addressed its core objectives regarding blue carbon pathways in coastal ecosystems. We demonstrated that elevated temperatures consistently restructure DOC composition in native macrophyte communities, notably reducing the recalcitrant fraction (by ~28% over 4 °C) while enhancing LDOC production. This occurred despite decreased DOC k, indicating a decline in the actual bioavailability of the warming-enhanced labile pool. In contrast, the presence of the invasive *Halophila stipulacea* had no meaningful short-term impact on metabolic rates or DOC fluxes. Furthermore, we developed and applied a standardized framework quantifying daily DOC production rates relative to plant biomass, carbon content in biomass, and chlorophyll content. This framework directly enables robust comparisons of DOC fluxes, particularly the crucial recalcitrant fraction, across macrophyte species with diverse morphologies and ecological strategies. By applying this carbon-based normalization at a global scale, we roughly estimate that macrophyte meadows convert a substantial amount of inorganic carbon into RDOC, comparable in magnitude, although 1.41 higher, to the carbon burial rates in the sediment. Our results, hence, underscore the potential contribution of RDOC produced by macrophyte communities to the long-term carbon storage, positioning RDOC production as a key, yet often overlooked, blue carbon pathway. Collectively, by fulfilling both objectives, our work refines blue carbon budgets and underscores the critical, yet climate-sensitive, role of DOC, particularly the recalcitrant fraction, in coastal carbon sequestration. The developed framework provides an essential tool for predicting how climate-driven changes in coastal vegetation will impact the ocean's long-term carbon storage capacity.

Reporting summary

Further information on research design is available in the Nature Portfolio Reporting Summary linked to this article.

Data availability

The datasets generated and analysed during this study, including the source data used to generate the figures and charts, are publicly available in the Zenodo repository at https://doi.org/10.5281/zenodo.18861550.

Code availability

Custom R scripts used for data processing, statistical analyses and figure generation are available in the same Zenodo repository as the study datasets at https://doi.org/10.5281/zenodo.18861550.

Received: 9 September 2025; Accepted: 9 March 2026;
Published online: 02 April 2026

References

1. Li, Z., Zhang, Y. G., Torres, M. & Mills, B. J. Neogene burial of organic carbon in the global ocean. *Nature* **613**, 90–95 (2023).
2. Jiménez-Ramos, R., Egea, L. G., D'Agostino, V. C., Degrati, M. & Loizaga, R. Carbon and nitrogen stocks in sediment at Península Valdés Biosphere Reserve: novel insights into the potential contribution of large marine vertebrates to carbon sequestration. *Front. Mar. Sci.* **12**, 1500594 (2025).
3. Kennedy, H. et al. Seagrass sediments as a global carbon sink: Isotopic constraints. *Glob. Biogeochemical Cycles* **24**, 1–8 (2010).
4. Duarte, C. M., Kennedy, H., Marbà, N. & Hendriks, I. Assessing the capacity of seagrass meadows for carbon burial: Current limitations and future strategies. *Ocean Coast. Manag.* **83**, 32–38 (2013).
5. Soto, N., Winters, G. & Antler, G. The effect of anaerobic remineralization of the seagrass *Halophila stipulacea* on porewater biogeochemistry in the Gulf of Aqaba. *Front. Mar. Sci.* **10**, 1250931 (2023).
6. Duarte, C. M. & Chiscano, C. L. Seagrass biomass and production: a reassessment. *Aquat. Bot.* **65**, 159–174 (1999).
7. Ortega, A. et al. Important contribution of macroalgae to oceanic carbon sequestration. *Nat. Geosci.* **12**, 748–754 (2019).
8. Filbee-Dexter, K. et al. Carbon export from seaweed forests to deep ocean sinks. *Nat. Geosci.* **17**, 552–559 (2024).
9. Gould, J., Bell, T. W. & Stubbins, A. Production and fate of macroalgal carbon in the ocean: How much do macroalgal organics matter?. *Limnol. Oceanogr. Lett.* **10**, 799–814 (2025).
10. Hansell, D. A., Carlson, C. A., Repeta, D. J. & Schlitzer, R. Dissolved Organic Matter in the Ocean: New Insights Stimulated by a Controversy. *Oceanography* **22**, 202–211 (2009).
11. Turner, J. T. Zooplankton fecal pellets, marine snow, phytodetritus and the ocean's biological pump. *Prog. Oceanogr.* **130**, 205–248 (2015).
12. Boyd, P. W., Claustre, H., Levy, M., Siegel, D. A. & Weber, T. Multi-faceted particle pumps drive carbon sequestration in the ocean. *Nature* **568**, 327–335 (2019).
13. Comstock, J. et al. Marine particle size-fractionation indicates organic matter is processed by differing microbial communities on depth-specific particles. *ISME Commun.* **4**, ycae090 (2024).
14. Friedlingstein, P. et al. Global carbon budget 2024. *Earth Syst. Sci. Data* **2024**, 1–133 (2024).
15. Álvarez-Salgado, X. A., Nieto-Cid, M., & Rossel, P. E. Dissolved organic matter. In Marine analytical chemistry (pp. 39−102). Cham: Springer International Publishing. (2022).
16. Hansell, D. A. Recalcitrant dissolved organic carbon fractions. *Annu. Rev. Mar. Sci.* **5**, 421–445 (2013).
17. Jiménez-Ramos, R. et al. Carbon metabolism and bioavailability of dissolved organic carbon (DOC) fluxes in seagrass communities are altered under the presence of the tropical invasive alga *Halimeda incrassata*. *Sci. Total Environ.* **839**, 156325 (2022).
18. Egea, L. G. et al. Effect of marine heat waves on carbon metabolism, optical characterization, and bioavailability of dissolved organic carbon in coastal vegetated communities. *Limnol. Oceanogr.* **68**, 467–482 (2023a).
19. Kubo, A. & Tanaka, H. Recalcitrant dissolved organic carbon release and production from aquatic plants leachate. *Mar. Pollut. Bull.* **189**, 114742 (2023).
20. Zhang, X. et al. Nutrient loading accelerates breakdown of refractory dissolved organic carbon in seagrass ecosystem waters. *Water Res.* **273**, 123017 (2025).
21. Yamuza-Magdaleno, A., Jiménez-Ramos, R., Cavijoli-Bosch, J., Brun, F. G. & Egea, L. G. Ocean acidification and global warming may favor blue carbon service in a *Cymodocea nodosa* community by modifying carbon metabolism and dissolved organic carbon fluxes. *Mar. Pollut. Bull.* **212**, 117501 (2025).
22. Brewer, P. G. & Peltzer, E. T. Depth perception: the need to report ocean biogeochemical rates as functions of temperature, not depth. *Philos. Trans. R. Soc. A: Math., Phys. Eng. Sci.* **375**, 20160319 (2017).
23. Lønborg, C., Álvarez–Salgado, X. A., Letscher, R. T. & Hansell, D. A. Large stimulation of recalcitrant dissolved organic carbon degradation by increasing ocean temperatures. *Front. Mar. Sci.* **4**, 436 (2018).
24. Hu, A. et al. Thermal responses of dissolved organic matter under global change. *Nat. Commun.* **15**, 576 (2024).
25. Lønborg, C., & Álvarez-Salgado, X. A. Recycling versus export of bioavailable dissolved organic matter in the coastal ocean and

efficiency of the continental shelf pump. *Glob. Biogeochem. Cycles*, **26**. https://doi.org/10.1029/2012GB004353 (2012).
26. Simone, M. N., Schulz, K. G., Oakes, J. M. & Eyre, B. D. Warming and ocean acidification may decrease estuarine dissolved organic carbon export to the ocean. *Biogeosciences* **18**, 1823–1838 (2021).
27. Barrón, C., Apostolaki, E. T. & Duarte, C. Dissolved organic carbon fluxes by seagrass meadows and macroalgal beds. *Front. Mar. Sci.* **1**, 11 (2014).
28. Bottino, F., Cunha-Santino, M. B. & Bianchini, I. Decomposition of particulate organic carbon from aquatic macrophytes under different nutrient conditions. *Aquat. Geochem.* **22**, 17–33 (2016).
29. Liu, S. et al. Nutrient loading diminishes the dissolved organic carbon drawdown capacity of seagrass ecosystems. *Sci. Total Environ.* **740**, 140185 (2020).
30. Moran, M. A. et al. The Ocean's labile DOC supply chain. *Limnol. Oceanogr.* **67**, 1007–1021 (2022).
31. Jiménez-Ramos, R. et al. Nutrient enrichment and herbivory alter carbon balance in temperate seagrass communities. *Mar. Pollut. Bull.* **206**, 116784 (2024).
32. Vilaplana, M. I. et al. The temperate seagrass species *Cymodocea nodosa* and the associated bacteria co-response to sunscreen pollution. *Mar. Environ. Res.* **208**, 107115 (2025).
33. Egea, L. G., Jiménez-Ramos, R., English, M. K., Tomas, F. & Mueller, R. S. Marine heatwaves and disease alter community metabolism and DOC fluxes on a widespread habitat-forming seagrass species (*Zostera marina*). *Sci. Total Environ.* **957**, 177820 (2024).
34. Bennett, E., Paine, E. R., Britton, D., Schwoerbel, J. & Hurd, C. L. The effect of temperature on rates of dissolved organic carbon (DOC) release by the kelp *Ecklonia radiata* (phylum Ochrophyta): Implications for the future coastal ocean carbon cycle. *J. Phycol. J. Phycol.* **60**, 1471–1484 (2024).
35. Graiff, A. et al. Differential effects of warming on carbon budget, photosynthetic yield and biochemical composition of cold-temperate and Arctic isolates of *Laminaria digitata* (Phaeophyceae). *J. Plant Physiol.* **306**, 154436 (2025).
36. Engel, A. et al. Effects of sea surface warming on the production and composition of dissolved organic matter during phytoplankton blooms: results from a mesocosm study. *J. Plankton Res.* **33**, 357–372 (2011).
37. Malinsky-Rushansky, N. Z. & Legrand, C. Excretion of dissolved organic carbon by phytoplankton of different sizes and subsequent bacterial uptake. *Mar. Ecol. Prog. Ser.* **132**, 249–255 (1996).
38. Bertilsson, S., Berglund, O., Pullin, M. J., & Chisholm, S. W. Release of dissolved organic matter by Prochlorococcus. *Vie et Milieu/Life & Environment*, 225−231 (2005).
39. Yamuza-Magdaleno, A., Jiménez-Ramos, R., Casal-Porras, I., Brun, F. G. & Egea, L. G. Long-term sediment organic carbon remineralization in different seagrass and macroalgae habitats: implication for blue carbon storage. *Front. Mar. Sci.* **11**, 1370768 (2024).
40. Chefaoui, R. M., Assis, J., Duarte, C. M. & Serrão, E. A. Large-scale prediction of seagrass distribution integrating landscape metrics and environmental factors: the case of *Cymodocea nodosa* (Mediterranean–Atlantic). *Estuaries Coasts* **39**, 123–137 (2016).
41. Beca-Carretero, P. et al. Climate change and the presence of invasive species will threaten the persistence of the Mediterranean seagrass community. *Sci. Total Environ.* **910**, 168675 (2024).
42. Thibaut, T. et al. Distribution of the seagrass *Halophila stipulacea*: A big jump to the northwestern Mediterranean Sea. *Aquat. Bot.* **176**, 103465 (2022).
43. Winters, G., Teichberg, M., Reuter, H., Viana, I. G. & Willette, D. A. Seagrasses Under Times of Change. *Front. Plant Sci.* **13**, 870478 (2022).
44. Conte, C., Apostolaki, E. T., Vizzini, S. & Migliore, L. A tight interaction between the native seagrass Cymodocea nodosa and the exotic *Halophila stipulacea* in the Aegean sea highlights seagrass holobiont variations. *Plants* **12**, 350 (2023).
45. Mannino, A. M., Balistreri, P., Mancuso, F. P., Bozzeda, F. & Pinna, M. Searching for the competitive ability of the alien seagrass *Halophila stipulacea* with the autochthonous species *Cymodocea nodosa*. *NeoBiota* **83**, 155–177 (2023).
46. Campbell, J. E., Allen, A. C., Sattelberger, D. C., White, M. D. & Fourqurean, J. W. First record of the seagrass *Halophila stipulacea* (Forsskal) Ascherson in the waters of the continental United States (Key Biscayne, Florida). *Aquat. Bot.* **196**, 103820 (2025).
47. Kashta, L. & Pizzuto, F. Sulla presenza di *Halophila stipulacea* (Forskål) Ascherson nelle coste dell'Albania. *Boll. delle sedute della Accad. Gioenia di Sci. Nat. Catania* **28**, 161–166 (1995).
48. Sghaier, Y. R., Zakhama-Sraieb, R., Benamer, I. & Charfi-Cheikhrouha, F. Occurrence of the seagrass *Halophila stipulacea* (Hydrocharitaceae) in the southern Mediterranean Sea. https://doi.org/10.1515/BOT.2011.061 (2011).
49. Aplikioti, M. et al. Further expansion of the alien seaweed *Caulerpa taxifolia* var. distichophylla (Sonder) Verlaque, Huisman & Procacini (Ulvophyceae, Bryopsidales) in the Eastern Mediterranean Sea. *Aquatic Invasions*, 11. https://doi.org/10.3391/ai.2016.11.1.02 (2016).
50. Wagner, S. et al. Soothsaying DOM: a current perspective on the future of oceanic dissolved organic carbon. *Front. Mar. Sci.* **7**, 341 (2020).
51. Egea, L. G., Jiménez–Ramos, R., Hernández, I. & Brun, F. G. Effect of In Situ short–term temperature increase on carbon metabolism and dissolved organic carbon (DOC) fluxes in a community dominated by the seagrass *Cymodocea nodosa*. *PloS one* **14**, e0210386 (2019a).
52. Paine, E. R. et al. Strong seasonal patterns of DOC release by a temperate seaweed community: Implications for the coastal ocean carbon cycle. *J. Phycol.* **59**, 738–750 (2023).
53. Morán, X. A. G., Gasol, J. M., Pedrós-Alió, C. & Estrada, M. Partitioning of phytoplanktonic organic carbon production and bacterial production along a coastal-offshore gradient in the NE Atlantic during different hydrographic regimes. *Aquat. Microb. Ecol.* **29**, 239–252 (2002).
54. Nagata, T. Production mechanisms of dissolved organic matter. *Microbial Ecol. Oceans*, **542**, 121−152 (2000).
55. Romera-Castillo, C., Sarmento, H., Alvarez-Salgado, X. A., Gasol, J. M. & Marrasé, C. Net production and consumption of fluorescent colored dissolved organic matter by natural bacterial assemblages growing on marine phytoplankton exudates. *Appl. Environ. Microbiol.* **77**, 7490–7498 (2011).
56. Kalbitz, K., Schmerwitz, J., Schwesig, D. & Matzner, E. Biodegradation of soil-derived dissolved organic matter as related to its properties. *Geoderma* **113**, 273–291 (2003).
57. Hansell, D. A. & Carlson, C. A. (Eds.). Biogeochemistry of marine dissolved organic matter. *Academic Press*. https://doi.org/10.1016/B978-0-12-405940-5.00011-X (2014).
58. Repeta, D., & Aluwihare, L. Chemical characterization and cycling of dissolved organic matter. In Biogeochemistry of marine dissolved organic matter (pp. 13-67). *Academic Press*. (2024).
59. Ruiz, H. & Ballantine, D. L. Occurrence of the seagrass *Halophila stipulacea* in the tropical west Atlantic. *Bull. Mar. Sci.* **75**, 131–135 (2004).
60. Willette, D. A. et al. Continued expansion of the trans-Atlantic invasive marine angiosperm *Halophila stipulacea* in the Eastern Caribbean. *Aquat. Bot.* **112**, 98–102 (2014).
61. Arona, A. et al. First record of the non-native seagrass *Halophila stipulacea* (Forsskål) Ascherson in Mallorca (Balearic Islands, Spain): Expanding its Western Mediterranean distribution. *Mediterranean Mar. Sci.* **27**, 108–115 (2026).

62. Winters, G. et al. The tropical seagrass *Halophila stipulacea*: reviewing what we know from its native and invasive habitats, alongside identifying knowledge gaps. *Front. Mar. Sci.* **7**, 300 (2020).
63. Picciotto, M., Bertuccio, C., Giacobbe, S. & Spanò, N. *Caulerpa taxifolia* var. distichophylla: a further stepping stone in the western Mediterranean. *Mar. Biodivers. Rec.* **9**, 73 (2016).
64. Egea, L. G., Jiménez-Ramos, R., Hernández, I. & Brun, F. G. Differential effects of nutrient enrichment on carbon metabolism and dissolved organic carbon (DOC) fluxes in macrophytic benthic communities. *Mar. Environ. Res.* **162**, 105179 (2020).
65. Peralta, G. et al. The morphometric acclimation to depth explains the long-term resilience of the seagrass *Cymodocea nodosa* in a shallow tidal lagoon. *J. Environ. Manag.* **299**, 113452 (2021).
66. Jiménez-Ramos, R. et al. Resistance and recovery of benthic marine macrophyte communities to light reduction: insights from carbon metabolism and dissolved organic carbon (DOC) fluxes, and implications for resilience. *Mar. Pollut. Bull.* **188**, 114630 (2023).
67. Egea, L. G. et al. Coupling carbon metabolism and dissolved organic carbon fluxes in benthic and pelagic coastal communities. *Estuar., Coast. Shelf Sci.* **227**, 106336 (2019b).
68. Casal-Porras, I. et al. Effects of a chronic impact on *Cymodocea nodosa* community carbon metabolism and dissolved organic carbon fluxes. *Sci. Total Environ.* **906**, 167740 (2024).
69. Stipcich, P. et al. Effects of high temperature and marine heat waves on seagrasses: Is warming affecting the nutritional value of *Posidonia oceanica*?. *Mar. Environ. Res.* **184**, 105854 (2023).
70. Beca-Carretero, P., Guihéneuf, F., Winters, G. & Stengel, D. B. Depth-induced adjustment of fatty acid and pigment composition suggests high biochemical plasticity in the tropical seagrass *Halophila stipulacea*. *Mar. Ecol. Prog. Ser.* **608**, 105–117 (2019).
71. Wellburn, A. R. The spectral determination of chlorophylls a and b, as well as total carotenoids, using various solvents with spectrophotometers of different resolution. *J. plant Physiol.* **144**, 307–313 (1994).
72. Winters, G. et al. Superior growth traits of invaded (Caribbean) versus native (Red sea) populations of the seagrass *Halophila stipulacea*. *Biol. Invasions* **25**, 2325–2342 (2023).
73. Barrón, C. & Duarte, C. M. Dissolved organic matter release in a *Posidonia oceanica* meadow. *Mar. Ecololy Prog. Ser.* **374**, 75–84 (2009).
74. Olivé, I., Silva, J., Costa, M. M. & Santos, R. Estimating seagrass community metabolism using benthic chambers: the effect of incubation time. *Estuaries Coasts* **39**, 138–144 (2016).
75. Duarte, C. M. et al. Seagrass community metabolism: Assessing the carbon sink capacity of seagrass meadows. *Glob. Biogeochemical Cycles* **24**, 1–8 (2010).
76. Barrón, C., Marbé, N., Terrados, J., Kennedy, H. & Duarte, C. M. Community metabolism and carbon budget along a gradient of seagrass (*Cymodocea nodosa*) colonization. *Limnol. Oceanogr.* **49**, 1642–1651 (2004).
77. Tuya, F., Png-Gonzalez, L., Riera, R., Haroun, R. & Espino, F. Ecological structure and function differ between habitats dominated by seagrasses and green seaweeds. *Mar. Environ. Res.* **98**, 1–13 (2014).
78. Egea, L. G., Jiménez-Ramos, R., Hernández, I., Bouma, T. J. & Brun, F. G. Effects of ocean acidification and hydrodynamic conditions on carbon metabolism and dissolved organic carbon (DOC) fluxes in seagrass populations. *PLoS ONE* **13**, e0192402 (2018a). 1−20.
79. Chen, J. et al. DOC dynamics and bacterial community succession during long-term degradation of *Ulva prolifera* and their implications for the legacy effect of green tides on refractory DOC pool in seawater. *Water Res.* **185**, 116268 (2020).
80. Zhang, T. & Wang, X. Release and microbial degradation of dissolved organic matter (DOM) from the macroalgae *Ulva prolifera*. *Mar. Pollut. Bull.* **125**, 192–198 (2017).
81. de los Santos, C. B. et al. Sedimentary organic carbon and nitrogen sequestration across a vertical gradient on a temperate wetland seascape including salt marshes, seagrass meadows and rhizophytic macroalgae beds. *Ecosystems* **26**, 826–842 (2023).
82. Jiménez-Arias, J. L. et al. Tidal elevation is the key factor modulating burial rates and composition of organic matter in a coastal wetland with multiple habitats. *Sci. Total Environ.* **724**, 138205 (2020).
83. Egea, L. G. et al. Comparison of macroplastics dynamic across a tidal-dominated coastal habitat seascape including seagrasses, salt marshes, rocky bottoms and soft sediments. *Mar. Pollut. Bull.* **196**, 115590 (2023b).
84. Olivé, I., Brun, F. G., Vergara, J. J. & Pérez-Lloréns, J. L. Effects of light and biomass partitioning on growth, photosynthesis and carbohydrate content of the seagrass *Zostera noltii* Hornem. *J. Exp. Mar. Biol. Ecol.* **345**, 90–100 (2007).
85. Olivé, I., Vergara, J. J. & Pérez-Lloréns, J. L. Photosynthetic and morphological photoacclimation of the seagrass *Cymodocea nodosa* to season, depth and leaf position. *Mar. Biol.* **160**, 285–297 (2013).
86. Georgiou, D., Alexandre, A., Luis, J. & Santos, R. Temperature is not a limiting factor for the expansion of *Halophila stipulacea* throughout the Mediterranean Sea. *Mar. Ecol. Prog. Ser.* **544**, 159–167 (2016).
87. Staehr, P. A. & Borum, J. Seasonal acclimation in metabolism reduces light requirements of eelgrass (*Zostera marina*). *J. Exp. Mar. Biol. Ecol.* **407**, 139–146 (2011).
88. Vaquer-Sunyer, R., Duarte, C. M., Jordà, G. & Ruiz-Halpern, S. Temperature dependence of oxygen dynamics and community metabolism in a shallow Mediterranean macroalgal meadow (*Caulerpa prolifera*). *Estuaries Coasts* **35**, 1182–1192 (2012).
89. Egea, L. G., Jiménez-Ramos, R., Vergara, J. J., Hernández, I. & Brun, F. G. Interactive effect of temperature, acidification and ammonium enrichment on the seagrass *Cymodocea nodosa*. *Mar. Pollut. Bull.* **134**, 14–26 (2018b).
90. Fogg, G. E. The ecological significance of extracellular products of phytoplankton photosynthesis. *Botanica Mar.* **26**, 3–14 (1983).
91. Duarte, C. M., Holmer, M. & Marbà, N. Plant–microbe interactions in seagrass meadows. *Interact. macro- Microorg. Mar. Sediment.* **60**, 31–60 (2005a).
92. Koch, M., Bowes, G., Ross, C. & Zhang, X. H. Climate change and ocean acidification effects on seagrasses and marine macroalgae. *Glob. change Biol.* **19**, 103–132 (2013).
93. Zimmerman, R. C., Smith, R. D. & Alberte, R. S. Thermal acclimation and whole-plantcarbon balance in Zostera marina L. (eelgrass). *J. Exp. Mar. Biologyand Ecol.* **130**, 93–109 (1989).
94. Terrados, J. & Ros, J. D. Temperature effects on photosynthesis and depth distribution of the seagrass *Cymodocea nodosa* (Ucria) Ascherson in a Mediterranean Coastal Lagoon: the Mar Menor (SE Spain). *Mar. Ecol.* **16**, 133–144 (1995).
95. Collier, C. J., Uthicke, S. & Waycott, M. Thermal tolerance of two seagrass species atcontrasting light levels: implications for future distribution in the Great Barrier Reef. *Limnol. Oceanogr.* **56**, 2200–2210 (2011).
96. Vogel, M. A., Mason, O. U. & Miller, T. E. Environmental stressors alter the composition of seagrass phyllosphere microbial communities. *Clim. Change Ecol.* **2**, 100042 (2021).
97. Joint, I. & Smale, D. A. Marine heatwaves and optimal temperatures for microbial assemblage activity. *FEMS Microbiol. Ecol.* **93**, fiw243 (2017).
98. Xie, Y. et al. Long-term response of the microbial community to the degradation of DOC released from *Undaria pinnatifida*. *Mar. Environ. Res.* **194**, 106313 (2024).
99. Chiquillo, K. L. et al. An invasive seagrass drives its own success in two invaded seas by both negatively affecting native seagrasses and benefiting from those costs. *Oikos* **2023**, e09403 (2023).

100. Steiner, S. C. C. & Willette, D. A. The expansion of *Halophila stipulacea* (Hydrocharitaceae, Angiospermae) is changing the seagrass landscape in the commonwealth of Dominica, Lesser Antilles. *Caribb. Naturalist* **22**, 1–19 (2015).
101. Winters, G., Nguyen, H. M. & Kaminer, M. Expansion of *Halophila stipulacea* in parallel with declines of native seagrasses in the eastern Mediterranean Sea. *Aquat. Bot.* **196**, 103829 (2025).
102. Wesselmann, M. et al. Seagrass (*Halophila stipulacea*) invasion enhances carbon sequestration in the Mediterranean Sea. *Glob. change Biol.* **27**, 2592–2607 (2021).
103. Holmer, M., Marbà, N., Lamote, M. & Duarte, C. M. Deterioration of sediment quality in seagrass meadows (*Posidonia oceanica*) invaded by macroalgae (*Caulerpa sp.*). *Estuaries coasts* **32**, 456–466 (2009).
104. Pedersen, M. O., Serrano, O., Mateo, M. A. & Holmer, M. Temperature effects on decomposition of a *Posidonia oceanica* mat. *Aquat. Microb. Ecol.* **65**, 169–182 (2011).
105. Maher, D. T., & Eyre, B. D. Benthic fluxes of dissolved organic carbon in three temperate Australian estuaries: Implications for global estimates of benthic DOC fluxes. *J. Geophys. Res.: Biogeosci.* **115**. https://doi.org/10.1029/2010JG001433 (2010).
106. Zeller, M. A. et al. The unique biogeochemical role of carbonate-associated organic matter in a subtropical seagrass meadow. *Commun. Earth Environ.* **5**, 681 (2024).
107. Liu, Y., Reible, D., Hussain, F. & Fang, H. Role of bioroughness, bioirrigation, and turbulence on oxygen dynamics at the sediment-water interface. *Water Resour. Res.* **55**, 8061–8075 (2019).
108. Blažina, M., Iveša, L. & Najdek, M. *Caulerpa racemosa*: adaptive varieties studied by fatty acid composition (Northern Adriatic Sea, Vrsar, Croatia). *Eur. J. Phycol.* **44**, 183–189 (2009).
109. Abal, E. G. et al. Physiological and morphological responses of the seagrass *Zostera capricorni* Aschers, to light intensity. *J. Exp. Mar. Biol. Ecol.* **178**, 113–129 (1994).
110. Bass, A. V., Falkenberg, L. J. & Thibodeau, B. Seagrasses under stress: Independent negative effects of elevated temperature and light reduction at multiple levels of organization. *Limnol. Oceanogr.* **70**, S448–S463 (2024).
111. Lønborg, C. et al. Depth dependent relationships between temperature and ocean heterotrophic prokaryotic production. *Front. Mar. Sci.* **3**, 90 (2016).
112. Lønborg, C., Davidson, K., Álvarez–Salgado, X. A. & Miller, A. E. Bioavailability and bacterial degradation rates of dissolved organic matter in a temperate coastal area during an annual cycle. *Mar. Chem.* **113**, 219–226 (2009).
113. Lønborg, C., Carreira, C., Jickells, T. & Álvarez-Salgado, X. A. Impacts of global change on ocean dissolved organic carbon (DOC) cycling. *Front. Mar. Sci.* **7**, 466 (2020).
114. Dinsdale, E. A. et al. Microbial ecology of four coral atolls in the Northern Line Islands. *PloS one* **3**, e1584 (2008).
115. Stepanauskas, R. N. et al. Bioavailability and sources of DOC and DON in macrophyte stands of a tropical coastal lake. *Hydrobiologia* **436**, 241–248 (2000).
116. Apostolaki, E. T. et al. Exotic *Halophila stipulacea* is an introduced carbon sink for the Eastern Mediterranean Sea. *Sci. Rep.* **9**, 9643 (2019).
117. Serrano, O., Almahasheer, H., Duarte, C. M. & Irigoien, X. Carbon stocks and accumulation rates in Red Sea seagrass meadows. *Sci. Rep.* **8**, 15037 (2018).
118. Yamuza-Magdaleno, A. et al. Dataset supporting "Temperature-driven decline in recalcitrant dissolved organic carbon weakens coastal macrophyte's blue carbon storage potential". Zenodo. https://doi.org/10.5281/zenodo.18861550 (2026).

Acknowledgements

This work has been funded with a Humboldt postdoc fellowship to Pedro Beca-Carretero, by the projects FINOCAME (PCM_00104.C17.I03), project co-financed by the Department of University, Research and Innovation of the Regional Government of Andalusia and by the European Union through the Next Generation EU funds of the Recovery, Transformation and Resilience Plan; DAME (PDC2021-120792-100), funded by the Ministry of Science and Innovation, the National Agency of Research, and the European Union (Next Generation EU Recovery Funds) Recovery, Transformation and Resilience Plan; and the SER-CADY project [FEDER-UCA18-107451], supported by the 2014–2020 ERDF Operational Programme and by the Department of Economic Transformation, Industry, Knowledge, and Universities of the Regional Government of Andalusia. Alba Yamuza-Magdaleno acknowledges a FPU grant from the Spanish Ministry of Science, Innovation and Universities. Pedro Beca-Carretero acknowledges support from the Alexander von Humboldt Foundation through a Humboldt Research Fellowship. Tomás Azcárate-García acknowledges a Severo Ochoa FPI predoctoral grant (PRE2020-096185) of the Spanish Ministry of Science, Innovation and Universities through the "Severo Ochoa Centre of Excellence" Institute of Marine Sciences (ICM-CSIC) of Barcelona (CEX2019-000928-S). We thank the Marine Experimental Ecology (MAREE) team at the ZMT, as well as L. Saige Alloway, for their support in developing the mesocosm. We are also grateful to A. Romero-Sánchez for his help with preparing the diagrams included in this paper. Thanks to the Integration and Application Network for the courtesy of supplying the vector symbols (ian.umces.edu/symbols/). We also thank to the anonymous referees for their constructive comments on an early version of the manuscript.

Author contributions

Alba Yamuza-Magdaleno: Conceptualization, Data Curation, Formal Analysis, Investigation, Methodology, Validation, Visualization, Writing - Original Draft Preparation, Writing - Review & Editing. Tomás Azcárate-García: Data Curation, Investigation, Methodology, Writing - Review & Editing. Luis G. Egea: Funding Acquisition, Methodology, Validation, Writing - Review & Editing. Xosé Antón Álvarez-Salgado: Data Curation, Methodology, Validation, Writing - Review & Editing. Hauke Reuter: Methodology, Project Administration, Resources, Writing - Review & Editing. Fernando G. Brun: Conceptualization, Funding Acquisition, Methodology, Resources, Supervision, Validation, Writing - Review & Editing. Pedro Beca-Carretero: Conceptualization, Data Curation, Funding Acquisition, Investigation, Methodology, Project Administration, Resources, Supervision, Validation, Writing - Original Draft Preparation, Writing - Review & Editing.

Competing interests

The authors declare that they have no known competing financial interests or personal relationships that could have appeared to influence the work reported in this paper.

Additional information

Supplementary information The online version contains supplementary material available at https://doi.org/10.1038/s43247-026-03417-y.

Correspondence and requests for materials should be addressed to Alba Yamuza-Magdaleno or Pedro Beca-Carretero.

Peer review information *Communications Earth & Environment* thanks Gloria Reithmaier and the other, anonymous, reviewer(s) for their contribution to the peer review of this work. Primary Handling Editors: Sophia Johannessen and Alice Drinkwater. A peer review file is available